Received Date : 28-Feb-2019
Revised Date : 02-Jun-2019
Accepted Date : 08-Jul-2019

Accepted Article

Benextramine and derivatives as novel human monoamine oxidases inhibitors: an integrated approach

Maria Luisa Di Paolo[1,2], Giorgio Cozza[1], Andrea Milelli[3], Francesca Zonta[4], Stefania Sarno[4], Elirosa Minniti[5], Fulvio Ursini[1], Michela Rosini[5], and Anna Minarini[5]
[1]*Department of Molecular Medicine, University of Padova, Padova, Italy, marialuisa.dipaolo@unipd.it*
[2] *Consorzio Interuniversitario "Istituto Nazionale Biostrutture e Biosistemi" Roma, Italy*
[3]*Department for Life Quality Studies, Alma Mater Studiorum-University of Bologna, Rimini, Italy*
[4]*Department of Biomedical Sciences, University of Padova, Padova, Italy*
[5]*Department of Pharmacy and Biotechnology, Alma Mater Studiorum-University of Bologna, Bologna, Italy*

Corresponding authors

Maria Luisa Di Paolo, Department of Molecular Medicine, Biological Chemistry section, Via G. Colombo 3, University of Padova, 35131 Padova, Italy; tel: ++39-049-8276119; e-mail: marialuisa.dipaolo@unipd.it; https://www.medicinamolecolare.unipd.it/

Anna Minarini, Department of Pharmacy and Biotechnology, Via Belmeloro 6, Alma Mater Studiorum-University of Bologna, 40126 Bologna, Italy; tel: ++39-051-2099709; anna.minarini@unibo.it; http://www.fabit.unibo.it/

Giorgio Cozza, Department of Molecular Medicine, Biological Chemistry section, Via G. Colombo 3, University of Padova, 35131 Padova, Italy; tel: ++39-049-8276154; e-mail: giorgio.cozza@unipd.it; https://www.medicinamolecolare.unipd.it/

Running title: Benextramine derivatives are MAOs inhibitors

Article type : Original Articles

Keywords: benextramine; monoamine oxidases; inhibitors; polyamines analogues, docking studies;

This article has been accepted for publication and undergone full peer review but has not been through the copyediting, typesetting, pagination and proofreading process, which may lead to differences between this version and the Version of Record. Please cite this article as doi: 10.1111/febs.14994
This article is protected by copyright. All rights reserved.

Accepted Article

Abbreviations: AD, Alzheimer's disease; BZA, benzylamine; DC_{50}: death concentration 50%; DMSO, dimethyl sulphoxide; DTT, 1,4-dithiothreitol; hr-MAO, human recombinant monoamine oxidase; MTDL, multi-target-directed ligand; NEM, *N*-ethylmaleimide; Par, pargyline; PD, Parkinson's disease; p-Tyr, p-tyramine; TMS, tetramethylsilane.

Abstract

The two human MAO isoforms (namely MAO A and MAO B) are enzymes involved in the catabolism of monoamines, including neurotransmitters, and for this reason are well-known and attractive pharmacological targets in neuropsychiatric and neurodegenerative diseases, for which novel pharmacological approaches are necessary. Benextramine is a tetraamine disulfide mainly known as irreversible α-adrenergic antagonist, but able to hit additional targets involved in neurodegeneration. As the molecular structures of monoamine oxidases contain nine cysteine residues, the aim of this study was to evaluate benextramine and eleven structurally related polyamine disulfides as potential MAO inhibitors. Most of the compounds were found to induce irreversible inactivation of MAOs with inactivation potency depending on both the polyamine structure and the enzyme isoform. The more effective compounds generally showed preference for MAO B. Structure-activity relationships studies revealed the key role played by the disulfide core of these molecules in the inactivation mechanism. Docking experiments pointed to Cys323, in MAO A, and Cys172, in MAO B, as target of this type of inhibitors thus suggesting that their covalent binding inside the MAO active site sterically impedes the entrance of substrate towards the FAD cofactor. The effectiveness of benextramine in inactivating MAOs was demonstrated in SH-SY5Y neuroblastoma cell line. These results demonstrated for the first time that benextramine and its derivatives can inactivate human MAOs exploiting a mechanism different from that of the classical MAO inhibitors and could be a starting point for the development of pharmacological tools in neurodegenerative diseases.

INTRODUCTION

Monoamine oxidases (MAOs) are mitochondrial FAD-containing enzymes that catalyse the oxidative deamination of biogenic amine neurotransmitters (dopamine, noradrenaline, adrenaline and serotonin), and a wide variety of xenobiotic amines, including therapeutic drugs.

The two MAO isoenzymes, MAO A and MAO B (70% of sequence identity), differ for their substrate specificities, inhibitor sensitivities and tissue localization [1, 2].

Being involved in the catabolism of neurotransmitters, MAOs are well-known pharmacological targets in various neurological, psychiatric and neurodegenerative diseases, such as Parkinson's disease (PD) and Alzheimer's disease (AD) [3, 4]. Indeed, MAO inhibitors decrease the catabolism of neurotransmitters and the subsequent generation of corresponding aldehydes, ammonia and hydrogen peroxide (reaction products), which have been linked to conditions of oxidative stress that can contribute to the onset of various diseases [5].

Different MAO inhibitors are or have been used in clinical practice as antidepressant and in the treatment of PD [6, 7]. Plenty of evidences suggest that the therapeutic potential of MAO inhibitors (such as deprenyl and rasagiline) are also related to their ability to hit other biochemical targets [8]. Indeed, their therapeutic actions in the treatment of neurodegenerative disorders have been linked to the reduction of the oxidative stress,

This article is protected by copyright. All rights reserved.

regulation of gene expression and induction of antiapoptotic and prosurvival factors [3, 4, 8-11]. The development of multi-target-directed ligands (MTDLs), such as ladostigil, able to hit simultaneously MAO B and acetylcholinesterase (AChE), strengthens their therapeutic potential in AD and other neurodegenerative disease [12, 13]. Additionally, in recent years MAOs (mainly MAO A) emerged as potential therapeutic targets in other pathologies, such as prostate cancer and cardiovascular diseases [14, 15], opening up new horizons for MAO inhibitors.

In search of novel types of MAO inhibitors, our previous studies highlighted that polyamine based analogues are capable to inhibit human MAOs [16, 17]. In particular, ITC-BzDD (*N*-benzyl-12-isothiocyanato-*N*-methyldodecan-1-amine) was found to act as MAO B competitive inhibitor, and as MAO A irreversible inhibitor (Fig.1) [17].

By exploring the molecular structure of MAOs, it emerged that both the isoforms contain nine Cys residues, one bound to the FAD-cofactor and eight in the reduced form: kinetic, structural and site-directed mutagenesis studies supported that some of these Cys may be important in maintaining the fully functional enzyme [18-20]. To probe the role of Cys residues on MAOs activity, the most used compounds were the "classical" *N*-ethylmaleimide (NEM) and its derivatives [19], and 2,2'dipiridyl disulfide [21]. Importantly, MAO A was generally found more easily inactivated by thiol oxidation compared to MAO B [19].

Given these premises, benextramine (**1**, Fig.1), characterized by a cystamine core in its structure, was herein selected to be studied on MAOs. Compound **1** is a tetraamine disulfide mostly known as an irreversible α-adrenergic antagonist [22-26], also able to hit additional targets involved in neurodegenerative processes, such as muscarinic receptors and AChE enzyme [27, 28]. It was demonstrated that compound **1** exerts its action towards the α-adrenergic receptor thanks to a disulfide-thiol interchange reaction between the disulfide moiety of the cystamine core and a Cys residue of the receptor, leading to a disulfide covalent bond formation. In this context, emerging studies emphasise the role of Cys residues as redox molecular switches in various signalling pathways and pathologies [29, 30], such as neurodegeneration [31]. Although compound **1** has been used as a template to design polyamine analogues as MTDLs against neurodegenerative diseases [27, 28], no data is available on its effects on MAOs.

Thus, the aim of this study was to evaluate compound **1** and a series of structurally related polyamine disulfides (**2-12**) (Table 1) as human MAO inhibitors. The results obtained by exploiting a multidisciplinary approach including kinetic studies integrated with docking experiments and *in cell* validation, showed that most of the tested compounds induced irreversible inactivation of both MAO isoforms. Compound **1** showed the highest k_{inact} value for MAO A, and the "short" analogue **12**, was found to be the most potent MAO B inactivator. By the comparison of the inactivation potency (k_{inact}/K_{IE}), compounds **1** and **9** were found to be MAO B selective. The importance of the disulfide bridge in the mechanism of inactivation of these molecules was demonstrated by testing carbon analogues of compound **1**. Docking experiments highlighted the role of Cys323 (in MAO A) and Cys172 (in MAO B) as targets of compound **1** and its derivatives. This investigation led to discovery of a new class of MAO inhibitors with an unprecedented mechanism of action. This discovery may have important implication in the design of new MAO inhibitors as therapeutic agents or bio-pharmacological investigation tools.

This article is protected by copyright. All rights reserved.

Accepted Article

RESULTS

Rational of compound selection

In order to investigate the structural features required for an optimal interaction of a polyamine disulfide scaffold with the MAO A and MAO B active sites, compound **1**, together with polyamine disulfide analogues **2-12,** (Table 1), were tested as potential MAO A and B substrates and inhibitors. The structural modifications applied to compound **1** concerned the variation of the length of the methylene linkers between the nitrogen atoms (compounds **2-5**), the replacement of the *o*-methoxybenzyl groups on the terminal amine functions with catechol (compound **6** and **9**), pyrrole (compound **8**) or pyridine (compound **7**) rings, and a decrease of the number of amine functions in the polyamine backbone, leading to the asymmetrically substituted triamine (compound **10**) and to diamines (compounds **11** and **12**). To boost the crucial role of the disulfide moiety in MAO interaction, Met-666 and methoctramine, two carbon analogue of compound **1** (Fig. 1) and the new diamine **13** (Table 1)**,** featuring the hydroxylated analogue of compound **1** truncated in two halves, were also included in the study.

Screening of the effects of compound 1 and its analogues on monoamine oxidase activity

To evaluate the potential effects of the polyamine analogues on human recombinant -MAOs (hr-MAOs), compounds **1-13** (Table 1) were firstly evaluated as potential substrates. No significant MAO activity was detected testing all the analogues in the 0.1-1 mM range of concentration, with the exception of the compound **10**, characterized by a free primary amino group. However, compound **10** behaved as a very poor substrate for MAO A (enzyme activity less than 1% compared to 1 mM, (*p*-Tyr).
Consequently, compounds **1-13,** Met-666 (carbon analogue of **1**)**,** cystamine (core moiety of **1**), and NEM (reference-standard reactive compound for thiols) were tested as potential inhibitors.
The kinetic parameters (K_m and V_{max}) of MAO A and MAO B were determined in the presence of 100 μM compounds added in the assay solution immediately before the substrate. The results are shown in Table 2 as the ratio between the V_{max} or K_m values with respect to control samples (in absence of any compounds). Most of these molecules affect both V_{max} and K_m, depending on the MAO isoform. The double-reciprocal plots reported as examples in Fig. 2 indicate that the most effective compounds decreased mainly MAO B substrate affinity (Fig. 2B) ($K_m/K_{m0} \approx 1.6$-2 with compounds **1** and **9** and $K_m/K_{m0} \approx 6$ with compound **4,** Table 2) whereas, in the case of MAO A, both the V_{max} and/or K_m values were affected (Fig. 2A). To understand the mechanism of action of these polyamine disulfides, their time-dependent inhibitory activity was investigated. MAOs were pre-incubated with 100 μM of each compound, in absence of substrate, and the residual enzyme activity was determined at various times, after dilution and addition of the substrate. Residual enzyme activity was mostly found to decrease with increasing incubation time, suggesting that most of the polyamine disulfides behaved as time-dependent MAO inactivators (see example of compound **1** in Fig 3 and the calculated apparent inactivation constant values, k_{obs}' in Table 2). Moreover, in our experimental conditions, these compounds were more potent than NEM and cystamine, being compounds **1, 4** and **12** the most effective molecules. In agreement with previous studies [19], NEM was found to inactivate MAO A faster than MAO B, whereas cystamine behaved as a very weak MAO B inactivator. Moreover, the substitution of the cystamine core of compound **10** with the ethanolamine moiety, leading to compound **13**, determined the loss of the inactivation capability toward both the MAO isoforms.

This article is protected by copyright. All rights reserved.

Concerning the length of the spacer between the inner and outer amine functions of the tetraamine backbone, compound **2** and **3**, respectively, the shorter and longer homologous of compound **1**, showed almost the same MAO inactivation profile. Increasing the length of the spacer up to 12 methylene units, as in compound **4**, resulted in a significant rise of the inactivation potency, suggesting that more hydrophobic chains boost the reactivity against MAOs. Elongation of the cystamine core of compound **2** with two methylene units led to compound **5**, resulting in a significant decrease of MAO inhibitory ability, particularly for MAO A, with an apparent inversion of selectivity (**5** is more effective on MAO B and compound **2** is more effective on MAO A). The replacement of the terminal *o*-methoxybenzyl groups of compound **1** with other aromatic rings resulted in a reduction of the activity: compound **7**, bearing the pyridine ring at the two terminal ends, is the less potent compound of the series. The substitution with a pyrrole ring has similar effect to that with the catechol ring (compound **6**) on MAO B; however, the introduction of the catechol moiety increased the selectivity for MAO B compared to the lead compound **1**. This apparent MAO B selectivity and decreased MAO A inhibitory activity was further enhanced in compound **9**, characterized both by a "lengthened" cystamine core and the catechol groups at the terminal ends.
The reduction in the number of amine functions in the polyamine backbone, as in the asymmetric triamine **10** and in the diamine **11**, decreased their inactivation capability mainly towards MAO A in comparison with compound **1**. Compound **12**, where the *o*-methoxybenzyl groups of compound **11** are replaced with *o*-methoxyphenoxyethyl moieties, turned out to be the second more potent compound in inactivating MAO B.
On this basis, compounds **1**, **4** and **12** (the most potent ones), compound **9** (the most selective for MAO B) and the triamine **10** were selected for a more detailed kinetic characterization as time-dependent inhibitors.

Kinetic characterization of the most potent and selective compounds

The inactivation rate constant values were determined at various concentrations of compounds **1**, **4**, **9**, **10** and **12** with both MAOs isoforms. From the plots k_{obs}' *vs* inhibitor concentrations, saturation kinetics were found with compounds **1**, **9, 10** and **12**. For these molecules, the two steps mechanism of inactivation, which consider a first step of formation of the reversible complex (EI) followed by the second step of the chemical reaction with the production of the irreversibly inactivated enzyme (E-X*) (Eqn.1-2, in Material and Methods), was found to fit the experimental data. In Fig. 4 the analysis of the kinetic data obtained with **1** *vs* MAOs (panels A-D) and with **12** *vs* MAO B (panels E,F) are shown as examples. The calculated k_{inact} (inactivation constant rate) and K_{IE} (inhibition constant that represents the enzyme-inhibitor dissociation constant) are reported in Table 3.
In the case of compound **4**, saturation was not reached (example in Fig. 4, panels G, H), thus, from the slope of the plots k_{obs}' *vs* inhibitor concentration, only the k_{inact}/K_{IE} parameter was calculated. Notably, also inactivation of MAO A by NEM showed a similar non-saturable behaviour (Fig. 4, panels I, J), in agreement with other studies [21]. Under our experimental conditions, inactivation of MAO A by NEM (k_{inact}/K_{IE} = 400 min^{-1} M^{-1}) is about one order of magnitude slower respect to compounds **1**, **4** and **12**.
From Table 3 it appears that all the tested compounds show higher affinity (lower K_{IE} values) for MAO B than for MAO A, resulting compound **1** the most potent MAO B inhibitor (K_{IE} = 6 μM for MAO B *vs* K_{IE} = 175 μM for MAO A). On the other side, the highest inactivation rate constants (at saturating concentration of compounds) were found with compound **12** (k_{inact} = 1.42 min^{-1} *vs* MAO B) and **1** (k_{inact} = 0.98 min^{-1} *vs* MAO A). Consequently, the best inhibitory potency (k_{inact}/K_{IE}), which represents the rate of inactivation under not-saturating

This article is protected by copyright. All rights reserved.

concentration of inhibitor, was found with compound **12** (k_{inact}/K_{IE} =109 x10^3 $M^{-1}min^{-1}$ *vs* MAO B), followed by compound **4** (k_{inact}/K_{IE} =51x10^3 $M^{-1}min^{-1}$ *vs* MAO A). By considering k_{inact}/K_{IE}, the most selective MAO B inhibitors were the catechol derivative **9** (MAO A:MAO B 1:27) and compound **1** (MAO A:MAO B 1:7), but only **1** maintained a high inactivation potency for both MAO isoforms.
The unsymmetrical substituted cystamine derivative **10**, lacking one of the *N*-(2-methoxybenzyl) hexanamine moieties of **1** was found to inactivate both MAOs with lower selectivity and potency than its precursor **1**. In particular, the k_{inact} value for MAO A is halved and its k_{inact}/K_{IE} for MAO B is decreased by a factor of 5, in comparison to **1.**

Inhibition and reversibility mechanisms of compound 1

To understand the role of the disulfide bond in inactivating MAOs, we focused our investigation on compound **1,** showing the best balance between selectivity and inhibitory potency *vs* MAO isoforms. After incubation and reduction with 1,4-dithiothreitol (DTT)**,** the disulfide bond of compound **1** was broken in half producing two molecules of thiols. The inactivation capability was tested by comparing the effect of 100 μM compound **1** and of 100 μM of DTT pre-reduced compound **1** on MAOs activity. Intriguingly, the products derived by the reduction of compound **1** inactivated MAO A and MAO B about 5 and 8 times faster, respectively than the entire molecule (Fig. 5).
To note that cystamine showed no increase in the inactivation rate constant *vs* MAOs after DTT treatment that led to cysteamine formation. These results suggested that the formation of a disulfide bond between the sulfhydryl group of the reduced form of compound **1** and a Cys residue of MAOs could be a possible mechanism of MAOs inactivation and that this interaction takes place faster with respect to the one with the entire disulfide molecule.
To evaluate the reversibility of the chemical bond between compound **1** and MAOs, the inactivated enzymes were extensively dialyzed. After dialysis, no recovery of MAO A activity was detected, whereas, in the case of MAO B, about 41% of activity was found (Table 4), suggesting that the irreversible inhibition induced by compound **1** versus MAO B is less efficient, as demonstrated also by the lower k_{inact} (see Table 3). The irreversible and partial reversible inactivation of MAO A and MAO B, respectively, were confirmed also by using compound **4**, bearing the longest chain within this series (data not shown)**.**
To note that, after inactivation by compound **1**, MAOs enzymatic activity was not recovered by DTT treatment (Table 4). This behaviour suggested that the disulfide bridge formed between compound **1** and a Cys of MAOs, could be buried, and, consequently, DTT-inaccessible.
To further confirm the role of the disulfide moiety of **1** in inactivating MAOs, Met-666, the carbon analogue of compound **1**, was assayed. Unlike compound **1**, if Met-666 is incubated with MAOs, a decrease in the enzyme activity over time was not observed (Table 2). Moreover, if tested without pre-incubation, Met-666 and compound **1** (100 μM) showed similar effects on K_m (Table 2, first columns). These results demonstrated that the substitution of the disulfide moiety of the irreversible inhibitor **1** with two methylene groups, as in Met-666, led to a weak reversible inhibitor of MAOs. In particular, Met-666 decreased V_{max} (K_I = 790 ± 190 μM) and increased K_m values (K_{EI}>1mM) of MAO A (Fig. 6A) and increased K_m values of MAO B (K_{EI} = 540 ± 130 μM (Fig. 6B)**.** Similar results were obtained also with methoctramine (Met-686, molecular structure in Fig. 1), another carbon analogue of **1**, characterized by an eight methylene inner chain.
All these data confirmed the key role played by the disulfide moiety in the irreversible mechanism of human MAO inactivation by compound **1.**

This article is protected by copyright. All rights reserved.

Accepted Article

Accepted Article

Protection experiments to prove that polyamine disulfides are "active-site-directed inhibitors"

The reported experimental evidence clearly demonstrated that compound **1** and its analogues inactivate MAOs through the disulfide moiety; however, it remains unclear if the mechanism of inactivation involves Cys located in the MAO active site and if the polyamine disulfides are to be considered active-site-directed inhibitors. To answer to this question, the ability of a competitive inhibitor or of a substrate to protect against compound **1** inactivation was evaluated [32].

First of all, inactivation by **1** was performed in the presence of the competitive inhibitor isatin [2, 33]. The apparent inactivation rate constant of MAOs (k'_{obs}) obtained with the lead compound **1** was slowed down in the presence of isatin (Table 5), by a factor of 6 and 4 in the case of MAO A and B, respectively. Similar results were obtained also with compound **4**, the longest analogue of the series.

Furthermore, the effect of the substrate on the inactivation rate was evaluated by using the compounds with the highest inactivation potency (k_{inact}/K_{IE}), compound **4** for MAO A**,** and compound **12** for MAO B. In the presence of saturating concentrations of substrate (1 mM *p*-Tyr for MAO A and 10 mM benzylamine for MAO B) both compounds **4** and **12** lost most of their capability to inactivate MAOs (Table 5).

These results strongly support the fact that the active site of MAOs is the main target of compound **1** and its analogues, thus involving Cys residues located in the catalytic cavity.

Docking studies

The above reported biochemical investigations suggested that the binding of compound **1, 4** and **12** might occur in the cavity of MAOs active site, through the formation of a covalent disulfide bond with a Cys of MAOs. With the aim to evaluate this hypothesis and to determine the binding mode of these compounds, docking studies were carried out using MAO A and MAO B crystal structures.

Before the docking procedure, a Site Finder strategy (see Material and Methods) was applied to select all the possible binding sites of MAO A and MAO B. Interestingly, in both cases the most suitable interaction zone was superimposed with the catalytic binding site of the two enzymes, accordingly to the mechanism of action of the molecules above discussed. The catalytic sites of both MAO A and MAO B are characterized by a hydrophobic tunnel and a small hydrophilic region located close to the FAD cofactor. Several cysteines are located inside the catalytic tunnel but only a couple of them are exposed towards the catalytic site, in particular, MAO A Cys323 and MAO B Cys172, located in the opposite side of the two cavities, are not conserved. Intriguingly, MAO A Cys323 (Thr314 in MAO B) is located in a motif almost identical except for the Cys to Thr substitution (MAO A: DYCG**C**MIIED; MAO B: DYCG**T**MIIDG); similarly, MAO B Cys172 (Asn171 in MAO A) belongs to a very conserved sequence (MAO B: FVNL**C**VTAE; MAO A: FVNI**N**VTSE). To note that even if one single cysteine is conserved in both MAO A and MAO B (Cys321 and Cys312, respectively), these amino acids are not accessible, accordingly to the Site finder approach. Indeed, MAO A Cys321 is shielded by Cys323 and Leu97, while MAO B Cys312 by Thr314 and Leu88.

To obtain structural information about the residues involved in the interaction inside the active site of MAOs and, since, under reductive conditions, compound **1** resulted in a more efficient MAO inactivator, compounds **1**, **9** and **12** were docked against MAO A and MAO B crystal structures as half-molecules, representing the thiol derivatives.

This article is protected by copyright. All rights reserved.

Docking results suggested that thiol molecules derived from the disulfide compounds **1** and **12** bind MAO A and MAO B active sites by exploiting two different hydrophobic cavities, located inside the tunnel, close each other but not superimposable. In particular, in MAO A, the two compounds insert their *o*-methoxybenzyl head into a hydrophobic region assembled by Pro113, Leu97, Ile 325 and the alkyl chain of Gln99 (Fig. 7A and C). On the other side, the aromatic heads of compounds **1** and **12** fit into a hydrophobic cavity built by Trp119, Leu164, Ile199, Leu167 in MAO B (Fig. 7B and D). While the heads of the two compounds are structurally conserved, sharing the same binding pocket in MAO A or in MAO B, the thiol tails present huge differences in length and chemical composition, thus reflecting an unrelated binding motif towards MAO A Cys323 and MAO B Cys172. Indeed, the shorter thiol chain of compound **12** is perfectly directed versus MAO A Cys323 by the hydrophobic interaction with Phe208 and Ile335, further stabilized by the hydrogen bond between the amino group of compound **12** and the carbonyl group of Phe208 (2.7 Å, Fig. 7A). In MAO B Ile316, Tyr326 and Leu171 address the sulfhydryl group of the thiol compound deriving from **12** towards Cys172 (Fig. 7B). Interestingly, the docking pose versus MAO B is partially superimposable with the crystallographic pose of pioglitazone (PDB code: 4A79, Fig S1 A*).* To note that the *in silico* pK values of the two complexes MAO A/compound **12** and MAO B/compound **12** are very similar (7.5 and 7.8, respectively).

On the contrary, the bulkier chain of compound **1** is not able to efficiently interact with MAO A Cys323 due to the short distance between Cys323 and the hydrophobic cavity bearing the methoxyphenyl ring of **1** (Fig. 7C). However, in the case of MAO B, compound **1** can easily accommodate his chain directing it versus Cys172, by exploiting the same hydrophobic interactions discussed for compound **12** (Fig. 7D). The difference binding poses of compound **1** against MAO A and B are reflected also on the *in silico* pK values. Indeed, while MAO A/**1** complex present a pK of 6.2, MAO B/**1** seems more efficient with a value (pK = 8.0) close to the one observed for MAO B/**12** complex.

In the case of compound **9**, the docking pose presents substantial differences. The substitution of the *o*-methoxyl group of the benzyl moiety with two hydroxyl groups drives the compound to interact in a more hydrophilic and deep region of MAO catalytic tunnel by performing direct contact with the FAD molecule (Fig. 7E and F). This interaction is further stabilized by hydrophobic contacts with MAO A Phe352 and Tyr407 as well as with MAO B Phe343 and Tyr398 (Fig. 7E and F). The thiol chain of compound **9** is directed versus MAO A Cys323 and MAO B Cys172, being the interaction with the first one (Fig. 7E), apparently less efficacious compared to the second one (Fig. 7F). This event is also reflected in the *in silico* pK values (MAO A/**9** pK = 6.5; MAO B/**9** pK = 7.1), even if they are close to the limit of significance cut off.

Interestingly, the *in silico* pK values above reported showed the same trends and selectivity as the K_{IE} determined by the kinetic approach: compound **12** binds with similar "affinity" to both MAOs, while compounds **1** and **9** show higher affinity for MAO B. To note that also the whole polyamine disulfides considered in the *in silico* analysis are able to bind to MAO A and MAO B. However, the pK values calculated suggested that the binding of the whole molecules to MAOs are less efficient compared to those of the corresponding thiols, supporting the results obtained in the biochemical experiments.

In summary, the docking results suggests that compounds **1**, **9** and **12** can efficiently interact with the catalytic sites of MAO A and MAO B, directing their thiol chains versus specific cysteines. To confirm the compatibility of the docking poses with the possible formation of a disulfide bridge, covalent docking has been performed for compound **1** versus MAO A and B (Fig. S1 B and C). The results obtained are superimposable with the previously reported for non-covalent docking; slight differences are explainable by the application of an optimization process to the final covalent complexes.

This article is protected by copyright. All rights reserved.

Accepted Article

Accepted Article

Toxicity evaluation and *in-cell* MAO inhibition of compound 1

After the kinetic and computational studies on the interaction of compound **1** and derivatives with human-recombinant MAOs, the effect of this novel type of MAO inhibitors on a suitable cellular model has been prioritized. Since the previously identified targets of compound **1** are involved in neurodegenerative diseases, the SH-SY5Y neuroblastoma cells, one of the most used model of neuronal function [34], were chosen as cellular model. To note that this cell line, as most of the neuronal cell models, expresses mainly MAO A [35] (see also https://www.proteinatlas.org). MAOs activity was preliminary tested in cellular lysates, using pre-incubation with clorgyline (irreversible and specific inhibitor of MAO-A) and pargyline (irreversible inhibitor of both MAO A and MAO B). Clorgyline was able to completely abolish MAOs activity, confirming that MAO A is the main type of MAO isoform expressed in SH-SY5Y cells, as previously reported [35].
Before evaluating the effect on MAOs activity, the cytotoxicity of the compounds was tested. The most efficient compounds **1** and **12** were used for these studies. Their effects were compared to that of methoctramine, a polyamine analogue lacking the disulfide moiety, already studied on the SH-SY5Y cells [36].
The cells were incubated for 12 and 24 h in the presence of increasing concentration of the above reported compounds and then the cell viability was determined. From the DC_{50} (Death Concentration 50) values calculated from plots shown in Fig. 8, it clearly appears that compound **1** has a much lower cytotoxic effect than compound **12** (DC_{50} = 252 ± 28 μM *vs* DC_{50} = 25 ± 7 μM and DC_{50} = 208 ± 10 μM *vs* DC_{50} = 22 ± 4 μM with compound **12**, at 12 and 24 h, respectively); the DC_{50} = 72 ± 10 μM obtained with methoctramine (at 24 h) was in good agreement with the previously reported value [36]. On this basis, only the less toxic compound **1**, was tested as potential MAO inhibitor on the cellular system; pargyline was also assayed as standard MAO inhibitor. After incubation of cells with compound **1** for 3 and 24 h, a significant decrease in MAOs activity was found (Fig. 9A). After 24 h, an IC_{50} of about 13 μM was found, a concentration too low to induce significant citotoxicity. No decrease in MAO A protein content was found by western blotting and immunostaining analysis (Fig. 9B). From Fig. 9B, an increase of about 30% of MAO A protein was observed at the highest compound **1** concentration (250 μM). An increase in MAO A expression was previously reported in the same cell line with other MAO inhibitors (selegiline and rasagiline, MAO B inhibitors) [37].
The above reported results confirm the effectiveness of compound **1** in the inactivation of MAO A in a cellular system, at not cytotoxic concentrations.

DISCUSSION

This study demonstrated for the first time that benextramine (**1**) and its derivatives can inactivate human MAO A and MAO B isoforms, exploiting a mechanism of inactivation different from that of the classical MAO inhibitors. While the traditional MAO inhibitors act by targeting the FAD cofactor, the mechanism herein proposed for benextramine involves a time-dependent inactivation by the formation of disulfide bridge with the thiol group of a Cys of the enzyme.
The inactivation rate constant values with compounds **1-13** were found dependent on: a) the polyamine disulfide skeleton, b) the aromatic substituent on the two terminal ends of the molecule and c) the MAO isoform. In particular, the *o*-methoxybenzyl moieties at the terminal ends of the tetraamine disulfide skeleton are responsible of a stronger potency than other substitutions; on the other side, the elongation of two methylene groups in the inner

This article is protected by copyright. All rights reserved.

cystamine core, decreases the inactivation potency *versus* MAO A to favour the selectivity towards MAO B.

By considering k_{inact}/K_{IE} (index of inactivation efficiency), the diamine **12**, the shortest analogue of the series, was found to be the most potent MAO B inactivator ($k_{inact}/K_{IE} = 1x10^5$ $M^{-1}min^{-1}$), and the tetraamine **4**, the longest one, appears to be the more potent MAO A inactivator ($k_{inact}/K_{IE} = 57x10^3$ $M^{-1}min^{-1}$); however, both the compounds are poorly selective. A good selectivity for MAO B was found for compounds **1** and **9** (MAO A: MAO B, 1:7 and 1:27, respectively).

By comparing these kinetic results with that previously found with ITC-BzDD (Fig. 1) [17], compounds **1**, **4** and **12** resulted more potent than ITC-BzDD as MAO A inactivator in terms of k_{inact}/K_{IE} or k_{inact}. Furthermore, although ITC-BzDD (Fig. 1) behaves with a different inhibition mechanism, that is as competitive inhibitor of MAO B, its K_{IE} value towards MAO B is comparable with those found with the inactivator compounds **1** and **12**.

Moreover, by comparing the kinetic behaviour of the standard and selective inhibitors targeting the FAD cofactor, clorgyline for MAO A and deprenyl for MAO B, **1** analogues show a lower inactivation efficiency (k_{inact}/K_{IE}, in the range 10^6-10^8 $M^{-1}min^{-1}$ for clorgyline and deprenyl *vs* k_{inact}/K_{IxE}, in the range 10^4-10^5 $M^{-1}min^{-1}$), but good inactivation rate constant values (k_{inact} about 0.9 min^{-1} with clorgyline and 0.08 min^{-1} with deprenyl *vs* k_{inact} = 1-1.4 min^{-1} with **1** and **12**). Additionally, the inactivation efficiency of **1** analogues is higher than that of other thiol reactive reagents (2,2'-dipyridyl disulfide, k_{inact}/K_i 1.2-0.3 x 10^3 M^{-1} min^{-1} for MAO A [21] and NEM, k_{inact}/Ki 0.4 x 10^3 M^{-1} min^{-1}). These data suggest that the mechanism of chemical inactivation by compound **1** derivatives could be considered as a potential new mode of inactivating MAOs.

The inactivation by compound **1** was found irreversible for MAO A and partially reversible for MAO B. This partial reversibility is probably explained by the stronger but reversible physical interaction of compound **1** with MAO B and by a concomitant slower chemical reactivity or reversibility of the chemical reaction (k_{inact} = 0.25 min^{-1} for MAO B *vs* 0.98 min^{-1} in MAO A).

By the comparison of the inhibitory behaviour of Met-666 *vs* compound **1** and compound **13** *vs* compound **10**, respectively, it was demonstrated the crucial role played by the disulfide bridge in the inactivation process. Indeed, in absence of this feature, inactivation did not occur and the compounds act as poor reversible inhibitor (Met-666), suggesting the formation of a disulfide bond between compound **1** and MAOs.

Previous structural studies demonstrated the presence of eight reduced Cys residues in both MAO proteins [19] and other authors reported that the mutation/chemical modification of some of them may affect enzyme activity [20, 21]; so the Cys residues of MAOs are the best candidates to react with the disulfide moiety of compound **1** and its derivatives.

The protection by inactivation in the presence of a competitive inhibitor or of a substrate strongly supported that these compounds target a Cys residue of MAO active site cavity. The docking experiments pointed to the not conserved Cys323 (in MAO A) and Cys172 (in MAO B) as targets (Fig. 7): the covalent disulfide bond formed between the molecules and these Cys residues of MAO active sites should impede/occlude the entrance of substrate towards the FAD-cofactor, resulting in enzyme inactivation.

However, alternative binding or additional binding to Cys at remote sites, such as on the enzyme surface, may not be excluded, even if the not recovery of enzyme activity, after DDT treatment suggests that the Cys involved in the binding of compound **1** and its analogues are solvent inaccessible.

This article is protected by copyright. All rights reserved.

Therefore, concerning the mechanism of MAO inactivation by compound **1** derivatives, two ways are here proposed: a) the pre-reduced disulfide (half-molecule of the compound) could react with the Cys of MAO active site via a sulfenic acid intermediate (–SOH), which might form inside the active site in air-exposed aqueous solutions [38]; b) the disulfide core of the compound could react with the Cys-SH of MAO active site through a classical reaction of thiol-disulfide interchange [38].
The first way is supported by the extremely efficacious enzyme inactivation by the DTT-reduced compounds **1** and **10**, which demonstrated that the free -SH groups formed are much more efficient than the whole disulfide-containing molecule in inactivating both MAOs. Under physiological conditions, in a cellular system, the presence of reducing agents, such as glutathione, could speed up the reduction of compound **1** analogues before reacting with MAO (bound to the mitochondrial membrane).
On the other side, the known flexibility of the molecular structure of the enzyme [40] and of the polyamine backbone might allow the disulfide compound/Cys interaction in the active site, through a thiol-disulfide interchange reaction, even if docking experiments suggested better binding affinities for the thiol compound (half molecule), compared to the disulfide. Indeed, these results could be impaired by the semiflexible docking protocol, in which the compounds enjoy full degree of freedom, while the protein is completely rigid and not subjected to induced fitting.
The efficacy of compound **1** in inactivating MAO A was confirmed also in a model of neuronal cells, where inactivation occurs at concentration one order of magnitude lower than its cytotoxic concentration (IC_{50} = 13 μM vs DC_{50} = 208 μM).

In conclusion, the main finding of this study is that human MAOs are novel targets for the tetraamine disulfide benextramine and its derivatives, exploiting a novel inactivation mechanism of MAOs.
Starting from the above reported results, further studies are in progress to design novel analogues with a better selectivity and reactivity than compound **1,** for a future potential development as pharmacological tools in neurodegenerative diseases.

MATERIALS AND METHODS

Chemicals and reagents

All chemicals were of analytical grade and purchased from Fluka-Sigma-Aldrich S.r.l. (Milan, Italy) with the exception of Amplex Red reagent (10-acetyl-3,7-dihydroxyphenoxazine), purchased from Molecular Probes/Invitrogen (Invitrogen s.r.l, San Giuliano Milanese (MI, Italy).
Human recombinant MAO A and MAO B expressed in baculovirus infected BT1 cells (5 mg/mL) and horseradish peroxidases were purchased from Fluka-Sigma-Aldrich s.r.l. (Italy). Rabbit polyclonal to MAO A was from Abcam and anti-βactin was from Sigma-Aldrich S.r.L. (Milan, Italy)

This article is protected by copyright. All rights reserved.

Accepted Article

Synthesis of compounds 1-13

Compounds **1-12** were synthesized following improved procedures respect to those previously reported [22-24, 26, 39]. We describe here the modified synthesis of compound **10** and the synthesis of the new compound **13** (Scheme 1). The detailed procedure is reported in the SI (NMR spectra in Fig.S2).
Briefly, 2-methoxybenzaldeyde was subjected to a classical reductive amination with 6-aminohexanol to furnish compound **14**. The secondary nitrogen was protected with Boc (**15**) and the hydroxy functionality was activated with tosyl chloride (**16**). Reaction between **16** and cystamine led to intermediate **17**, which was subjected to acidic deprotection to remove Boc group giving compound **10** as hydrochloride salt. Reaction between **16** and ethanolamine led to compound **18**, which was subjected to acidic deprotection to give compound **13** as hydrochloride salt. Benextramine can be obtained adopting the same procedure described for **17**, by using **16** and cystamine in 2:1 equivalent ratio, followed by deprotection of Boc groups.

Monoamine oxidase activity experiments

Amine oxidase assay methods

Amine oxidase activity was determined by measuring H_2O_2 generation rate by a peroxidase-coupled continuous assay. The Amplex Red reagent was used as fluorogenic substrate for horseradish peroxidase [40]. No significant interference of the various polyamine analogues on fluorescence intensity was observed.
All experiments were carried out in 50 mM Hepes-NaOH, 50 mM KCl, 120 mM NaCl, pH 7.4 and at 37°C.
Assays were carried out in a final volume of 800 μl, in the presence of Amplex Red (100 μM) and horseradish peroxidase type II (5 UmL^{-1}). Benzylamine (BZA) and p-tyramine (*p*-Tyr) were used as substrates for MAO B and MAO A, respectively. Initial velocities were determined by measuring the increase in fluorescence intensity (λ_{exc} = 563 nm and λ_{em} = 586 nm); H_2O_2 generation rate was calculated from the change in fluorescence intensity, by means of calibration curves obtained by serial dilution of stock solution of H_2O_2. In particular, since the fluorescence intensity generated by the system peroxidase-Amplex Red-hydrogen peroxide, decreases in the presence of high tyramine concentrations, the reaction rates of MAO A, at various tyramine concentrations, were calculated using specific calibration curves built for each concentration of the substrate used for the enzyme activity assay. If not differently reported, hr-MAO A and hr-MAO B concentrations in the assay solutions were 3 and 6 μg/ml, respectively.
In experiments carried out in the presence of DTT, which was found to interfere with the Amplex Red- peroxidase assay method, MAO activity was determined by the method using kynuramine as substrate [41]. Briefly: enzyme stock solutions, after incubation in the presence of DTT (with or without inhibitor), were diluted with assay buffer to get a final concentration 0.003 mg/mL for MAO-A and 0.006 mg/mL for MAO-B; 300 μM kynuramine (final concentration) was added to the 200 μl of assay solution (0.1 M potassium phosphate buffer, pH 7.4, 0.1 mM EDTA). After 30 min incubation at 37°C, the reaction was stopped by addition of 2 M NaOH (80 μl) and 480 μL of distilled water. Kynuramine deaminated by MAO spontaneously cyclizes to give 4-hydroxyquinoline, the amount of which was determined by the fluorescence intensity of the peak of its emission spectra (λ_{exc} = 330 nm and

This article is protected by copyright. All rights reserved.

λ_{em} 330-530 nm), using a specific calibration curve built with the standard 4-hydroxyquinoline.
This kynuramine assay was also used for the assay of MAO activity in SH-SY5Y cell lysates (25 μL of cell lysates in 200 μL of the assay solution). MAO activity was expressed as $pmol_{4HQ}$ min^{-1} $mg_{protein}^{-1}$. To verify the presence of MAO A activity in this cells, SH-SY5Y lysates, were pre-incubated for 15 min at 37 °C with clorgyline (1 μM, to inhibit MAO A) and pargyline (250 μM, to inhibit both MAO A and MAO B); then the substrate (kynuramine) was added and the residual MAO activity was determined.

Inactivation of MAOs by compound 1 pre-treated with DTT

Compound **1** (1mM) was pre-incubated with DTT (20 mM) in Hepes buffer (pH 7.4) for 15 min at 37°C. In these conditions, the disulfide bond is reduced breaking compound **1** in two half-molecules characterized by the presence of thiol groups. After reduction, experiments of inactivation of MAOs were carried out using 100 μM of compound **1**, or 100 μM of DTT-reduced compound **1**. MAOs without any compounds and MAOs with only DTT (at 2 mM final concentration, as in the sample with the reduced compound **1**), were run under the same experimental conditions and were taken as control samples. MAOs activity studies were carried out using the assay method with kynuramine as substrate.
The effect of DTT-oxidation product on MAOs, was evaluated using DTT-pretreated cystamine under the same experimental conditions.

Reversibility experiments

MAO A and MAO B (0.025 mg/mL) were incubated in the presence of compound **1** or **4** 200 μM. When the residual activity was decreased and constant at its minimum value (about zero for MAO A and about 30%, in the case of MAO B), the samples were extensively dialyzed against several changes of buffer (100 mM potassium phosphate, pH 7.20, at 4 °C). Control samples of MAOs were run simultaneously, under the same experimental conditions. After dialysis, the residual MAO activity and protein concentration were determined, to calculate the residual specific activity ($nmol_{H2O2}$ min^{-1} $mg^{-1}_{protein}$).
The reversibility was also tested by adding DTT to the MAOs previously inactivated by **1**. DTT was added at a final concentration of 10 mM, for about 20 min, at 36°C. The residual enzyme activity was tested after dilution (1:40) of the enzyme- **1** solution, before adding substrate. Control samples of enzyme, in the presence and absence of DTT were also run and treated under the same experimental conditions to verify the effect of DTT on the free enzyme.

Protein assay

The protein content of samples was measured by the Bradford method, with bovine serum albumin as standard [42].

This article is protected by copyright. All rights reserved.

In silico analysis

The crystal structure of human MAO A and MAO B were retrieved from the Protein Data Bank (PDB codes: 2Z5X and 4A79, respectively) and processed in order to remove ligands and water molecules. Hydrogen atoms were added to the protein structures using standard geometries with the MOE program [43]. To minimize contacts between hydrogens, the structures were subjected to Amber99 force-field minimization until the rms (root mean square) of conjugate gradient was <0.1 kcal•mol^{-1}•Å^{-1} (1 Å = 0.1 nm) keeping the heavy atoms fixed at their crystallographic positions. Compound **1**, and the selected derivatives **12** and **9** were built using MOE, considering the molecules in both oxidized and reduced states; Gasteiger partial charges (MOE Suite) were added.
Before the molecular docking procedure a Site Finder Approach [43] was performed; this tool, by identifying regions of tight atomic packing (using Alpha Shapes, a generalization of convex hulls developed in [44], allows the identification of pockets and surface sites and was successfully applied in different target analysis [45, 46]. In the case of MAO A and MAO B, the procedure suggests a cavity, superimposable with the catalytic tunnel of both the enzymes, as the best interaction zone for the molecules considered in this work.
Using the Site Finder indications, a preparation step for the docking procedure was performed with Glide package (Schrodinger suite) [47]. A set of co-crystallized inhibitors of MAO A and MAO B were used to optimize the docking protocol, determining a final Glide grid (outer grid dimensions: 14Å x 28Å x 16Å for MAO A; 18Å x 25Å x 15Å for MAO B). Compounds **1, 12** and **9** were docked in the defined sites and grids by using the XP (extra precision) procedure. The *in silico* association constant (pK), estimated using MOE suite, was optimized exploiting the crystal structures available during the docking preparation phase. It is expressed as the summation of a directional hydrogen-bonding term, a directional hydrophobic interaction term, and an entropic term; higher values indicate more affinity with a significance cut off of 0.5.
Covalent docking of compound **1** versus MAO A and MAO B was performed by using CovDock tool [47]. The optimization of the final covalent complexes was performed using Prime [47].

Cell cultures

Human SH-SY5Y neuroblastoma cells (A.T.C.C., Manassas, VA) were cultured in DMEM medium (Sigma-Aldrich) supplemented with 10% fetal bovine serum, 2 mM L-glutamine, 100 U/mL penicillin and 100 mg/mL streptomycin (Sigma-Aldrich) and maintained in a 5% CO_2 humidified atmosphere at 37 °C and grown until they reached 70% confluence for a maximum of 20 passages.
After cell treatment with the various compounds, cells were gathered, washed with phosphate saline buffer (PBS) and after centrifugation pellets were lysated in 20 mM Hepes-NaOH, pH 7.5, 1mM ethylenediaminetetraacetic acid (EDTA) and protease inhibitor cocktail (about 10 million cells/1mL of lysis buffer) and frozen in liquid nitrogen. Samples were stored at -80 °C until use.

This article is protected by copyright. All rights reserved.

Accepted Article

Cell viability assay

Log-phase cells were seeded into the 96-wells plate (15.000 cells/well) and were allowed for the attachment overnight followed by the treatment with increasing concentrations of compound **1** and methoctramine for 12 h and 24 h. Cellular proliferation was quantified with colorimetric methods based on the metabolic reduction of the soluble yellow 3-(4,5-dimethylthiazol-2-yl)-2,5-diphenyltetrazolium bromide (MTT) dye to its insoluble formazan [48]. The absorbance was read on Titertek Multiskan Plus plate reader (Flow Laboratories, Sutton, U.K.) using 540 nm wavelength.
Results were normalized to time point zero (t = 0 h), and the concentration inducing 50% of cell death (DC_{50}) was calculated with respect to DMSO treated controls, with Prism 7.0a software.

Western blot analysis

Cells treated at the reported concentrations of **1** and pargyline for 3h and 24h were trypsinized and lysed by addition of 20 mM Hepes (pH 7.5), 1 mM EDTA and protease and phosphatase inhibitor cocktails and frozen in liquid nitrogen. Protein concentration was determined by the Bradford method. 30 μg of protein lysates were subjected to 9% SDS-PAGE, blotted on Immobilon-P membranes (Merck-Millipore), processed in western blot with the indicated primary antibodies and detected by enhanced chemiluminescent detection system (ECL). Re-probing of a blot with new primary antibodies was done after 3 washing with phosphate buffered saline with 0.1% Tween-20 (Sigma-Aldrich).
Immunostained bands were quantified by means of a Kodak-Image-Station 4000MM-PRO and analysis with Carestream Molecular Imaging software (New-Haven, CT).
Differences among treatments were evaluated by analysis of variance (ANOVA) followed by Bonferroni post-test, using Prism 7.0a; $p<0.05$ was considered significant.

Kinetic and statistical analysis

Steady-state kinetic parameters (V_{max} and K_m) were calculated by fitting the Michaelis-Menten equation to the experimental data (initial rate of reactions *vs* substrate concentrations) by non-linear regression analysis, with Sigma Plot software, version 9.0 (Jandel Scientific, San Rafael, CA, USA) and the value of the kinetic parameter obtained from the best fit and its S.E. are reported.

Time-dependent inhibition studies. Recombinant MAO A and MAO B (0.02-0.05 mg/mL) in the Hepes buffer, were pre-incubated for periods from 0 to about 50 minutes, at 37 °C in the presence and in the absence of inhibitor (control sample). After various time intervals of pre-incubation (at least 5 times after mixing of enzyme and inhibitor), the residual MAOs enzyme activity of samples was determined: an aliquot of sample was withdrawn and diluted in the assay buffer (50-fold dilution) and, after 1 minute, substrate was added under "saturating" condition, (*p*-Tyr 1 mM and BZA 10 mM for MAO A and B, respectively).
All time-dependent inhibition experiments were monitored relative to a control sample, which was run exactly as the experiment except without inhibitor added (only an equivalent volume of solvent used for the tested inhibitor, was added).

This article is protected by copyright. All rights reserved.

The enzyme activity of this control sample (v_0) was set to 100% and for each time point the ratio between residual enzyme activities (v_{+I}) relative to the control sample (v_0), was calculated. The "apparent inactivation rate constant" values (k_{obs}'), for each inhibitor concentration, were calculated by linear regression analysis of the data of logarithm of residual activity ($\ln (v_{+I}/v_0)$) *versus* time. The k_{obs}' values were plotted *versus* [I] and, in the case of a saturation behaviour, the Kitz and Wilson model, shown in the following equation, was found to be appropriate to fit the time-dependent inhibition data (k_{obs}' *vs* inhibitor concentration):

$$E + I \underset{}{\overset{K_{EI}}{\rightleftharpoons}} EI \xrightarrow{k_{inact}} EI^* \quad (1)$$

In this scheme, a rapid reversible interaction between free enzyme (E) and inhibitor (I) is followed by a slower, irreversible reaction, which transforms the reversible enzyme-inhibitor complex (EI) into an irreversible enzyme inhibitor complex (EI*). The inactivation rate constant (k_{inact}) and the enzyme-inhibitor dissociation constant (K_{IE}), were calculated by fitting eqn. 2 to the data of "apparent inactivation rate constants" (k_{obs}') *versus* $[I]_0$ (non-linear regression analysis, with Sigma Plot software, version 9.0)

$$k_{obs}' = k_{inact}[I]_0 / (K_{EI} + [I]_0) \quad (2)$$

If saturation kinetics is not observed, only the apparent bimolecular rate constant k_{inact}/K_{IE} was calculated from the slope of the plot of k_{obs}' against $[I]_0$.
Unless stated otherwise, the correlation coefficient for linear regression was 0.98 or greater.
All experiments were repeated independently at least three times, and the experimental data were expressed as the mean ± standard deviation (SD).
Statistical analyses of data from cellular experiments were conducted using Student's t-test. Values of $*p < 0.05$ or $**p < 0.01$ were defined as statistically significant. All analyses were carried out with the GraphPad Prism program (GraphPad Software, Inc., San Diego, CA). Error bars on all graphs consider 95% confidence intervals.
For calculating the IC_{50} value of compound **1** in the cellular system, curve fitting was performed by non-linear regression analysis using the standard "dose-response" curve equation and the Sigma Plot software.

Acknowledgments The Authors thank the "International Polyamine Foundation - ONLUS" for the availability to look up in the Polyamines documentation and the Modelling Section (MMS, University of Padova) for the kind support.
This research was supported by institutional grants from the University of Padova, Italy (60A06-1707/15 to M.L.D.P. and COZZ_SID18_01 to G.C.) and by the institutional grant from the University of Bologna, Italy "University of Bologna - RFO" to A.M.

Conflict of interest: the authors declare they have no conflicts of interests with the contents of this article.

This article is protected by copyright. All rights reserved.

Accepted Article

Accepted Article

Author contributions

MLDP, AM (Anna Minarini) and GC, conceived the project; MLDP conducted all kinetic investigations, analysed all the results and wrote the manuscript; GC conducted the computational studies, analysed and discussed all the results and participated in writing the manuscript; AM (Andrea Milelli) contributed to the synthesis of compounds and to writing the paper; FZ carried out cell cultures and analysis of cellular data; SS contributed to design and analyse all cellular experiments; EM carried out the synthesis of compounds; FU contributed to the analysis and discussion of the results; MR contributed to the analysis of results; AM (Anna Minarini) designed the compounds, carried out their synthesis, analysed and discussed all the results and participated in writing the manuscript. All authors have given approval to the final version of the manuscript.

References

1. Edmondson DE & Binda C (2018) Monoamine Oxidases. *Subcell Biochem* **87**, 117-139.
2. Binda C, Li M, Hubalek F, Restelli N, Edmondson DE & Mattevi A (2003) Insights into the mode of inhibition of human mitochondrial monoamine oxidase B from high-resolution crystal structures. *Proc Natl Acad Sci U S A* **100**, 9750-9755.
3. Cai Z (2014) Monoamine oxidase inhibitors: promising therapeutic agents for Alzheimer's disease (Review). *Mol Med Rep* **9**, 1533-1541.
4. Youdim MB, Edmondson D & Tipton KF (2006) The therapeutic potential of monoamine oxidase inhibitors. *Nat Rev Neurosci* **7**, 295-309.
5. Bortolato M, Chen K & Shih JC (2008) Monoamine oxidase inactivation: from pathophysiology to therapeutics. *Adv Drug Deliv Rev* **60**, 1527-1533.
6. Finberg JP (2014) Update on the pharmacology of selective inhibitors of MAO-A and MAO-B: focus on modulation of CNS monoamine neurotransmitter release. *Pharmacol Ther* **143**, 133-152.
7. Fisar Z (2016) Drugs related to monoamine oxidase activity. *Prog Neuropsychopharmacol Biol Psychiatry* **69**, 112-124.
8. Szoko E, Tabi T, Riederer P, Vecsei L & Magyar K (2018) Pharmacological aspects of the neuroprotective effects of irreversible MAO-B inhibitors, selegiline and rasagiline, in Parkinson's disease. *J Neural Transm (Vienna)* **125**, 1735-1749.
9. Youdim MB, Bar Am O, Yogev-Falach M, Weinreb O, Maruyama W, Naoi M & Amit T (2005) Rasagiline: neurodegeneration, neuroprotection, and mitochondrial permeability transition. *J Neurosci Res* **79**, 172-179.
10. Weinreb O, Amit T, Bar-Am O & Youdim MB (2007) Induction of neurotrophic factors GDNF and BDNF associated with the mechanism of neurorescue action of rasagiline and ladostigil: new insights and implications for therapy. *Ann N Y Acad Sci* **1122**, 155-168.
11. Weinstock M, Kirschbaum-Slager N, Lazarovici P, Bejar C, Youdim MB & Shoham S (2001) Neuroprotective effects of novel cholinesterase inhibitors derived from rasagiline as potential anti-Alzheimer drugs. *Ann N Y Acad Sci* **939**, 148-161.
12. Ramsay RR & Tipton KF (2017) Assessment of Enzyme Inhibition: A Review with Examples from the Development of Monoamine Oxidase and Cholinesterase Inhibitory Drugs. *Molecules* **22**.
13. Weinreb O, Amit T, Bar-Am O & Youdim MB (2016) Neuroprotective effects of multifaceted hybrid agents targeting MAO, cholinesterase, iron and beta-amyloid in ageing and Alzheimer's disease. *Br J Pharmacol* **173**, 2080-2094.

This article is protected by copyright. All rights reserved.

14. Deshwal S, Di Sante M, Di Lisa F & Kaludercic N (2017) Emerging role of monoamine oxidase as a therapeutic target for cardiovascular disease. *Curr Opin Pharmacol* **33**, 64-69.
15. Wu JB, Shao C, Li X, Li Q, Hu P, Shi C, Li Y, Chen YT, Yin F, Liao CP, et al. (2014) Monoamine oxidase A mediates prostate tumorigenesis and cancer metastasis. *J Clin Invest* **124**, 2891-2908.
16. Bonaiuto E, Minarini A, Tumiatti V, Milelli A, Lunelli M, Pegoraro M, Rizzoli V & Di Paolo ML (2012) Synthetic polyamines as potential amine oxidase inhibitors: a preliminary study. *Amino Acids* **42**, 913-928.
17. Bonaiuto E, Milelli A, Cozza G, Tumiatti V, Marchetti C, Agostinelli E, Fimognari C, Hrelia P, Minarini A & Di Paolo ML (2013) Novel polyamine analogues: from substrates towards potential inhibitors of monoamine oxidases. *Eur J Med Chem* **70**, 88-101.
18. Wu HF, Chen K & Shih JC (1993) Site-directed mutagenesis of monoamine oxidase A and B: role of cysteines. *Mol Pharmacol* **43**, 888-893.
19. Hubalek F, Pohl J & Edmondson DE (2003) Structural comparison of human monoamine oxidases A and B: mass spectrometry monitoring of cysteine reactivities. *J Biol Chem* **278**, 28612-28618.
20. Vintem AP, Price NT, Silverman RB & Ramsay RR (2005) Mutation of surface cysteine 374 to alanine in monoamine oxidase A alters substrate turnover and inactivation by cyclopropylamines. *Bioorg Med Chem* **13**, 3487-3495.
21. Weyler W & Salach JI (1985) Purification and properties of mitochondrial monoamine oxidase type A from human placenta. *J Biol Chem* **260**, 13199-13207.
22. Melchiorre C, Yong MS, Benfey BG & Belleau B (1978) Molecular properties of the adrenergic alpha receptor. 2. Optimum covalent inhibition by two different prototypes of polyamine disulfides. *J Med Chem* **21**, 1126-1132.
23. Quaglia W, Brasili L, Cristalli G, Giardina D, Picchio MT & Melchiorre C (1988) Structure-activity relationships among benextramine-related tetraamine disulfides. Chain length effect on alpha-adrenoreceptor blocking activity. *J Med Chem* **31**, 1861-1866.
24. Ueda Y, Melchiorre C, Lippert B, Belleau B, Chona S & Triggle DJ (1978) Molecular properties of the adrenergic alpha-receptor. I--Structural requirements for specific covalent occupancy by N,N'-bis--(5-aminopentyl)cystamine derivatives. *Farmaco Sci* **33**, 479-495.
25. Angeli P, Brasili L, Brancia E, Giardina D, Quaglia W & Melchiorre C (1985) Structure-activity relationships among benextramine-related tetraamine disulfides at peripheral alpha-adrenoreceptors. *J Med Chem* **28**, 1643-1647.
26. Giardina D, Brasili L, Melchiorre C, Belleau B & Benfey BG (1981) Molecular properties of the adrenergic a-receptor. 6. Optimum carbon chain-length between the inner nitrogen and the sulfur of tetramine disulfides. *Eur J Med Chem - Chimica Therapeutica* **16** 569-571.
27. Melchiorre C, Bolognesi ML, Minarini A, Rosini M & Tumiatti V (2010) Polyamines in drug discovery: from the universal template approach to the multitarget-directed ligand design strategy. *J Med Chem* **53**, 5906-5914.
28. Minarini A, Milelli A, Tumiatti V, Rosini M, Bolognesi ML & Melchiorre C (2010) Synthetic polyamines: an overview of their multiple biological activities. *Amino Acids* **38**, 383-392.
29. Fra A, Yoboue ED & Sitia R (2017) Cysteines as Redox Molecular Switches and Targets of Disease. *Front Mol Neurosci* **10**, 167.
30. Rossin F, Villella VR, D'Eletto M, Farrace MG, Esposito S, Ferrari E, Monzani R, Occhigrossi L, Pagliarini V, Sette C, et al. (2018) TG2 regulates the heat-shock response by the post-translational modification of HSF1. *EMBO Rep* **19**.

This article is protected by copyright. All rights reserved.

Accepted Article

31. Minarini A, Milelli A, Tumiatti V, Rosini M, Simoni E, Bolognesi ML, Andrisano V, Bartolini M, Motori E, Angeloni C, et al. (2012) Cystamine-tacrine dimer: a new multi-target-directed ligand as potential therapeutic agent for Alzheimer's disease treatment. *Neuropharmacology* **62**, 997-1003.
32. Plapp BV (1982) Application of affinity labeling for studying structure and function of enzymes. *Methods Enzymol* **87**, 469-499.
33. Hubalek F, Binda C, Khalil A, Li M, Mattevi A, Castagnoli N & Edmondson DE (2005) Demonstration of isoleucine 199 as a structural determinant for the selective inhibition of human monoamine oxidase B by specific reversible inhibitors. *The Journal of biological chemistry* **280**, 15761-15766.
34. Xicoy H, Wieringa B & Martens GJM (2017) The SH-SY5Y cell line in Parkinson's disease research: a systematic review. *Mol Neurodegener* **12**, 10.
35. Fitzgerald JC, Ufer C, De Girolamo LA, Kuhn H & Billett EE (2007) Monoamine oxidase-A modulates apoptotic cell death induced by staurosporine in human neuroblastoma cells. *Journal of neurochemistry* **103**, 2189-2199.
36. Zini M, Passariello CL, Gottardi D, Cetrullo S, Flamigni F, Pignatti C, Minarini A, Tumiatti V, Milelli A, Melchiorre C, et al. (2009) Cytotoxicity of methoctramine and methoctramine-related polyamines. *Chem Biol Interact* **181**, 409-416.
37. Inaba-Hasegawa K, Akao Y, Maruyama W & Naoi M (2013) Rasagiline and selegiline, inhibitors of type B monoamine oxidase, induce type A monoamine oxidase in human SH-SY5Y cells. *J Neural Transm (Vienna)* **120**, 435-444.
38. Nagy P (2013) Kinetics and mechanisms of thiol-disulfide exchange covering direct substitution and thiol oxidation-mediated pathways. *Antioxid Redox Signal* **18**, 1623-1641.
39. Chiarini A, Minarini A, Budriesi R & Melchiorre C (1990) Molecular properties of the histamine H2-receptor. Covalent inhibition by tetraamine disulfides. *Farmaco* **45**, 1001-1011.
40. Zhou M & Panchuk-Voloshina N (1997) A one-step fluorometric method for the continuous measurement of monoamine oxidase activity. *Anal Biochem* **253**, 169-174.
41. Santillo MF, Liu Y, Ferguson M, Vohra SN & Wiesenfeld PL (2014) Inhibition of monoamine oxidase (MAO) by beta-carbolines and their interactions in live neuronal (PC12) and liver (HuH-7 and MH1C1) cells. *Toxicol In Vitro* **28**, 403-410.
42. Bradford MM (1976) A rapid and sensitive method for the quantitation of microgram quantities of protein utilizing the principle of protein-dye binding. *Anal Biochem* **72**, 248-254.
43. Molecular Operating Environment (MOE 2010.10) CCG, Inc, 1255 University St., Suite 1600, Montreal, Quebec, Canada, H3B 3X3.
44. Edelsbrunner H (1955) Smooth surfaces for multi-scale shape representation, . *Foundations of Software Technology and Theoretical Computer Science* **Springer Berlin, Heidelberg**, 391–412
45. Cozza G, Zanin S, Sarno S, Costa E, Girardi C, Ribaudo G, Salvi M, Zagotto G, Ruzzene M & Pinna LA (2015) Design, validation and efficacy of bisubstrate inhibitors specifically affecting ecto-CK2 kinase activity. *Biochem J* **471**, 415-430.
46. Cozza G, Rossetto M, Bosello-Travain V, Maiorino M, Roveri A, Toppo S, Zaccarin M, Zennaro L & Ursini F (2017) Glutathione peroxidase 4-catalyzed reduction of lipid hydroperoxides in membranes: The polar head of membrane phospholipids binds the enzyme and addresses the fatty acid hydroperoxide group toward the redox center. *Free Radic Biol Med* **112**, 1-11.
47. Friesner RA, Banks JL, Murphy RB, Halgren TA, Klicic JJ, Mainz DT, Repasky MP, Knoll EH, Shelley M, Perry JK, et al. (2004) Glide: a new approach for rapid, accurate docking and scoring. 1. Method and assessment of docking accuracy. *J Med Chem* **47**, 1739-1749.

This article is protected by copyright. All rights reserved.

Accepted Article

48. Twentyman PR, Fox NE & Rees JK (1989) Chemosensitivity testing of fresh leukaemia cells using the MTT colorimetric assay. *Br J Haematol* **71**, 19-24.

Supporting information

Additional supporting information may be found online in the Supporting Information section at the end of the article.

Synthesis of compounds **10** and **13**.

Fig. S1. Superimposition between compound **12** and pioglitazone in MAO B; covalent docking of benextramine (**1**) against MAOs.

Fig. S2. NMR spectra of compounds **10** and **13**.

A) ^{1}H and ^{13}C NMR spectra of compound **10**

B) ^{1}H and ^{13}C NMR spectra of compound **13**

Accepted Article

This article is protected by copyright. All rights reserved.

Table 1. Molecular structures of benextramine (1) and its analogues.

Compound	Structure
Benextramine (1)	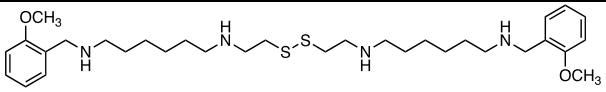
	Modification of the length of methylene linkers between the amino groups
2	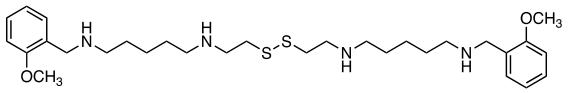
3	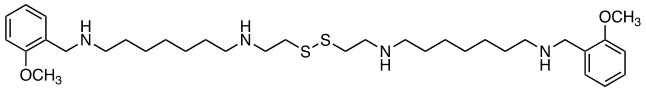
4	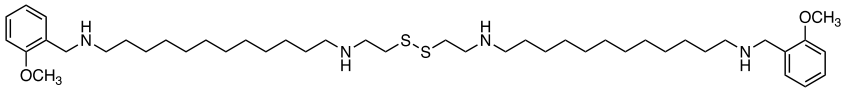
	Elongation of the cystamine core
5	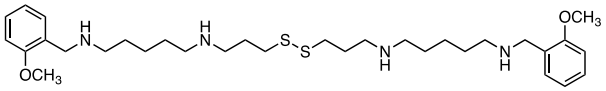
	Replacemtent of the o-methoxybenzyl groups
6	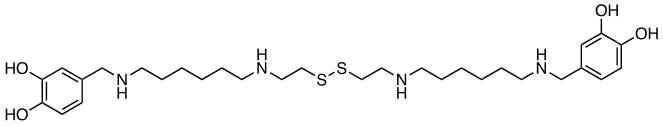
7	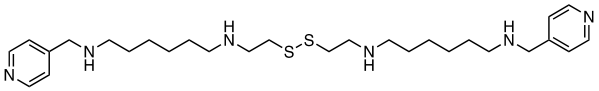
8	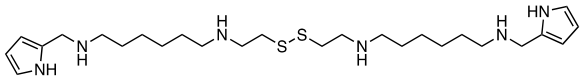
9	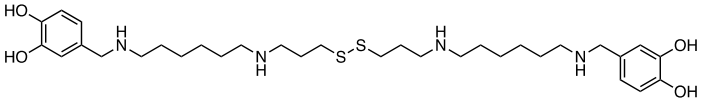
	Decrease in the number of amino groups
10	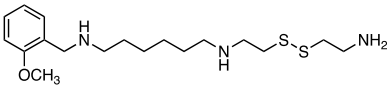
11	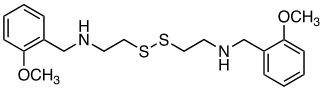

Accepted Article

This article is protected by copyright. All rights reserved.

12	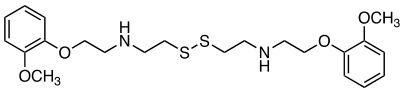
	Replacement of the disulfide core
13	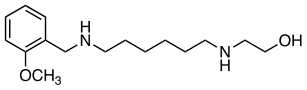
MET666	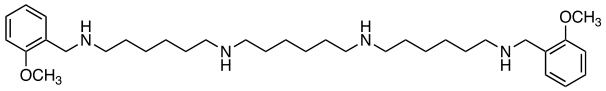
Cystamine	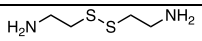
NEM	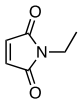

For each group of molecules, a brief description of the rational modifications is reported. The reference compounds cystamine (core moiety) and NEM (-SH reactive compound) are also shown.

Accepted Article

This article is protected by copyright. All rights reserved.

Table 2. Preliminary screening of compounds 1-13 as potential inhibitors *vs* hr-MAOs.

Compounds	hr-MAO A		hr-MAO B		hr-MAO A	hr-MAO B
(100 μM)	V_{max}/V_{max0}	K_m/K_{m0}	V_{max}/V_{max0}	K_m/K_{m0}	k_{obs}' (min^{-1})	k_{obs}' (min^{-1})
1	0.77	1.5	0.90	1.89	0.350±0.039	0.217±0.031
Effect of the length of methylene linkers between the nitrogen atoms						
2	0.85	0.9	0.95	2.21	0.387±0.012	0.197±0.070
3	0.78	1.23	0.72	2.02	0.378±0.043	0.105±0.027
4	n.d.[(a)]	n.d. [(a)]	0.47	6.3	5.8±1.0	2.43±0.50
Effect of the elongation of the cystamine core						
5	0.93	1.28	0.88	1.55	0.054±0.005	0.118±0.003
Effect of the replacement of the o- methoxybenzyl groups						
6	1.0	1.20	1	1.2	0.039±0.003	0.060±0.06
7	1.04	1.20	1	2.02	0.017±0.002	0.003±0.01
8	1.0	1.10	1.0	1.20	0.077±0.010	0.078±0.013
9	1.0	1.7	1	1.6	0.024±0.005	0.284±0.100
Effect of the decrease in the number of amine functions						
10	0.76	1.08	0.92	1.25	0.207±0.027	0.176±0.020
11	0.87	0.8	1	1.14	0.166±0.017	0.33 ±0.10
12	0.64	0.94	0.77	1.87	0.450±0.105	0.940±0.280
Effect of the replacement of the disulfide core						
13	0.90	1.10	1	1.10	0.003±0.002[(b)]	0.001±0.001
Met-666	1	1.5	1	1.74	0.003±0.002[(b)]	0.001±0.001
CYSTAMINE	1	1	1	1	0.002±0.001[(b)]	0.010±0.002
NEM	1	1	0.8	1.2	0.027±0.003	0.005±0.002

Steady-state kinetic parameters in the absence of compounds were: $Vmax_{0,p\text{-Tyr}} = 110 \pm 9$ nM/min and $Km_{0,p\text{-Tyr}} = 165 \pm 30$ for MAO A; $Vmax_{0,BZA} = 109 \pm 11$ nM/ and $Km_{0,BZA} = 280 \pm 45$ for MAO B. The "apparent inactivation rate constant" values (k_{obs}') of the various compounds for MAOs were determined by the linear regression analysis of data of residual activity ($\ln(v_{+I}/v_o)$ *vs* time)($r \geq 0.98$). Parameter ± S.D are reported (n=3)

[(a)] n.d.: not determinable, MAO A was immediately inactivated.

[(b)] k_{obs}' equivalent to that of control samples in absence of compound

This article is protected by copyright. All rights reserved.

Table 3. Inactivation rate constant and inhibition constant values of the most effective polyamine disulfides.

Compound	MAO A			MAO B			Selectivity MAO A/MAO B	
	k_{inact} (min^{-1})	K_{IE} (μM)	k_{inact}/K_{IE} ($M^{-1}min^{-1}$)	k_{inact} (min^{-1})	K_{IE} (μM)	k_{inact}/K_{IE} ($M^{-1}min^{-1}$)	k_{inact}	k_{inact}/K_{IE}
1	0.98±0.01	175±14	5.6±0.1 x10^3	0.25±0.01	6.3±0.6	40.0± 0.4 x10^3	3.9:1	1:7.1
4	n.d.	n.d.	51 ±7 x$10^{3(a)}$	n.d.	n.d.	18.3±6 x$10^{3(a)}$	n.d.	2.8:1
9	0.04±0.01	77±25	0.5±0.1 x10^3	0.19±0.01	14±2	13.8±1.0 x10^3	1:4.8	1:27
10	0.40±0.01	97±9	4.0±0.5 x10^3	0.22±0.01	30±5	7.8± 1.7 x10^3	1.8:1	1:1.9
12	0.57±0.04	20±4	28.0±7.0 x10^3	1.42±0.06	13±2	109.0±17.0 x10^3	1:2.5	1:3.9

The kinetic parameters of inactivation were calculated fitting equation 2 to experimental data (k'_{obs} of inactivation *vs* inhibitor concentrations), by non-linear regression analysis (parameter ± standard error values are shown).
n.d.: not determinable, saturation was not reached in the explored compound **4** concentration range (2-100 μM)
[(a)]This parameter is the slope value obtained by the linear regression of the data of the plot k'_{obs} *vs* compound **4** concentrations.

This article is protected by copyright. All rights reserved.

Table 4. Irreversibility of the inactivation of MAOs by compound 1

	RECOVERED MAO ACTIVITY (%)	
A) Effect of dialysis on MAOs inactivated by compound 1		
Sample	**hr-MAO A**	**hr-MAO B**
Control	100[a]	100[b]
Compound 1-inactivated MAO	0	41±5
B) Effect of DTT on MAOs inactivated by compound 1		
Control	100	100
Control + DTT	87±6	110±11
Compound 1-inactivated MAO	0	36±4
Compound 1- inactivated MAO after DTT	0	24±4

A) *Effect of dialysis*: MAOs were inactivated by compounds **1 (**200 μM) and then extensively dialyzed; after dialysis, the recovered MAO activity was measured. A control MAO samples was run under the same experimental conditions.
B) *Effect of DTT*: MAO A and MAO B were inactivated by pre-incubation with compound **1** (200 μM for 15 min at 36°C); then DTT 10 mM was added. After additional 20 min of incubation, samples were diluted and the residual MAO activity was tested, using the kynuramine assay method (final concentration in the assay: compound **1** 5 μM and DTT 0.25 mM)
Means ±SD are shown (n=3).
[a] MAO A specific activity: 30 nmol min^{-1} $mg_{protein}^{-1}$
[b] MAO B specific activity: 16 nmol min^{-1} $mg_{protein}^{-1}$

This article is protected by copyright. All rights reserved.

Table 5. Protective effect of a competitive inhibitor and of the substrate on inactivation of MAOs by compounds 1 and its derivatives.

A) Effect of the competitive inhibitor Isatin					
Enzyme	**[Compound]**	**[Isatin][a]** (μM)	**k_{obs}' (min^{-1})**		**k_{obs}' / $k_{obs'+ISATIN}$**
	[1]		- isatin	+ isatin	
MAO A	100 μM	100	0.350±0.039	0.060±0.005	5.8
MAO B	100 μM	12	0.217±0.031	0.057±0.007	3.8
	[4]				
MAO A	100 μM	100	5.8±1.4	3.0±0.3	2
MAO B	100 μM	12	2.35±0.52	0.52±0.08	4.5

B) Effect of the substrate				
Enzyme	**[Compound]**	**Substrate**	**k_{obs}' (min^{-1})**	
	[**4**]		- substrate	+ substrate
MAO A	5 μM	*p*-Tyr	0.92±0.14	0.53±0.07
MAO B	5 μM	BZA	0.31±0.03	No inactivation
	[**12**]			
MAO A	5 μM	*p*-Tyr	0.349±0.08	No inactivation
MAO B	5 μM	BZA	0.105±0.01	No inactivation

A) *Effect of the competitive inhibitor isatin on inactivation by compound **1** and **4**.* Inactivation experiments were performed under standard conditions, in the presence and absence of isatin.

B) *Effect of substrate on inactivation of MAOs by compounds **4** and **12**.* Inactivation experiments were performed under the standard conditions, in the presence and absence of substrate ([S]>>Km: 1 mM *p*-Tyr for MAO A and 10 mM BZA)

The "apparent inactivation rate constant" values (k_{obs}') for MAOs were determined by linear regression analysis of data of residual activity ($\ln(v_{+I}/v_o)$) *vs* time. Error bars represent the SD of the parameters (n = 3 replicates).

[a)] Isatin concentrations were 6-7 times higher than its corresponding K_I for the free enzyme ([E-Isatin]/[E]>6). In our experimental conditions: Ki = 16±3 μM and Ki = 2.3±0.5 μM for MAO A and MAO B, respectively, in agreement with those previously reported [33].

This article is protected by copyright. All rights reserved.

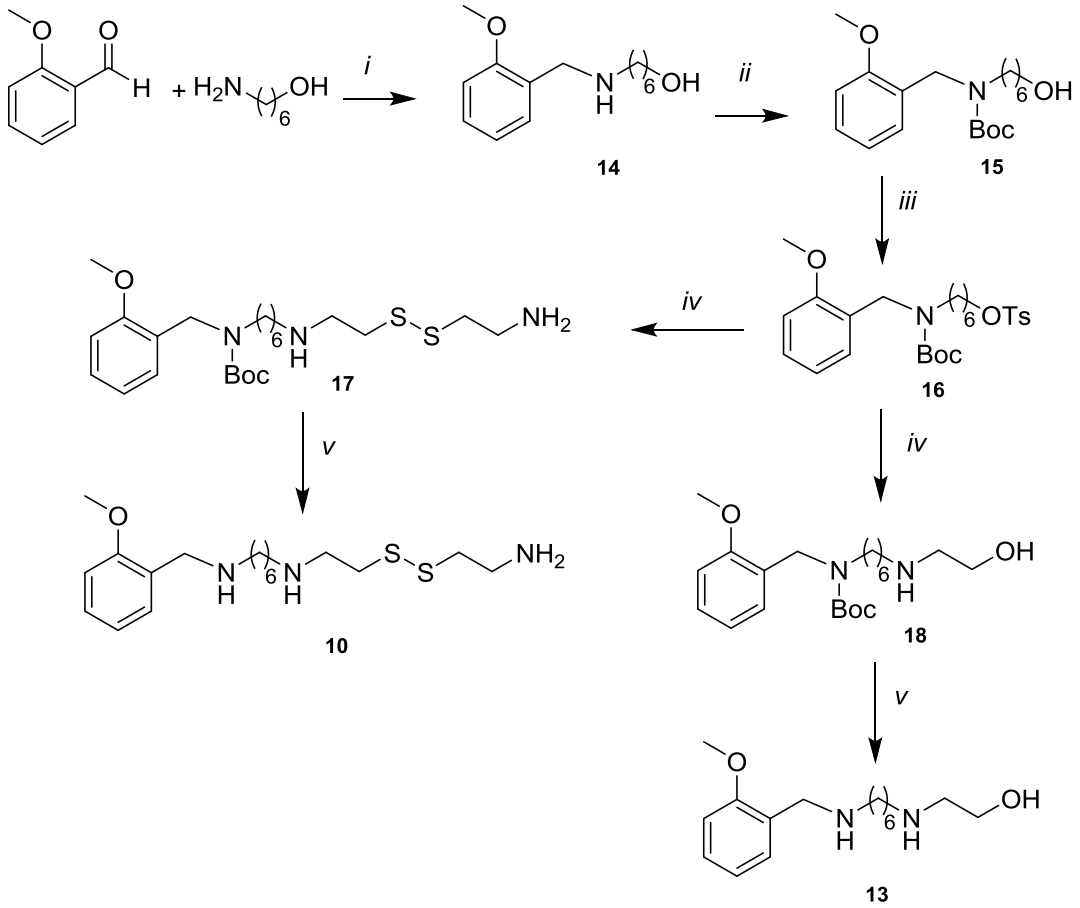

Scheme 1. *i*) a. *o*-OMe-benzaldehyde, EtOH, reflux, 5 h, b. $NaBH_4$, EtOH, rt, , 16h,79% yield; *ii*) Boc_2O, CH_2Cl_2, rt, 16 h, quantitative yield; *iii*) tosyl chloride, Et_3N, DMAP, CH_2Cl_2, 0 °C, 1.5 h, 81% yield; *iv*) cystamine (for **17**) or ethanolamine (for **18**), DMF, Et_3N, rt, 3 days, 36-60% yield; *v*) 4M HCl/dioxane, 0 °C, 40 min, 81% yield. Boc = $-COOC(CH_3)_3$; Ts = $-SO_2C_6H_4CH$

Accepted Article

This article is protected by copyright. All rights reserved.

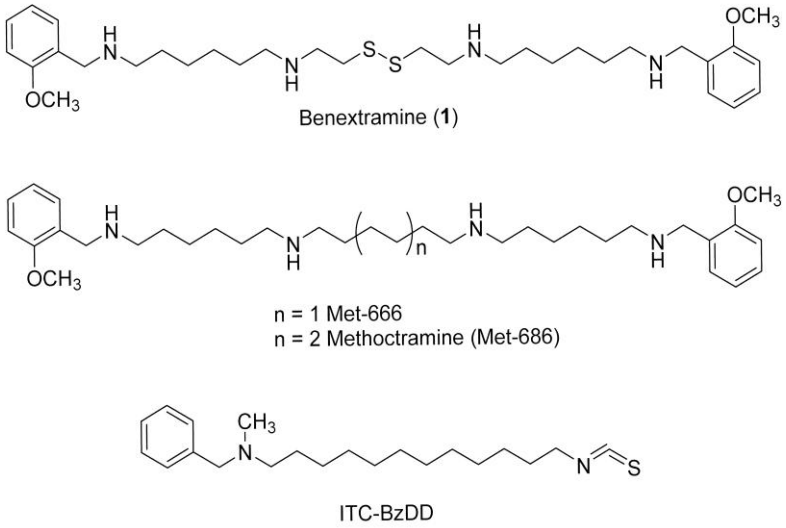

Fig. 1. Structures of the prototype of the tetraamine disulfides, benextramine (**1**), its carbon analogues (Met-666 and methoctramine) and of the previously studied MAO inhibitor ITC-BzDD [17].

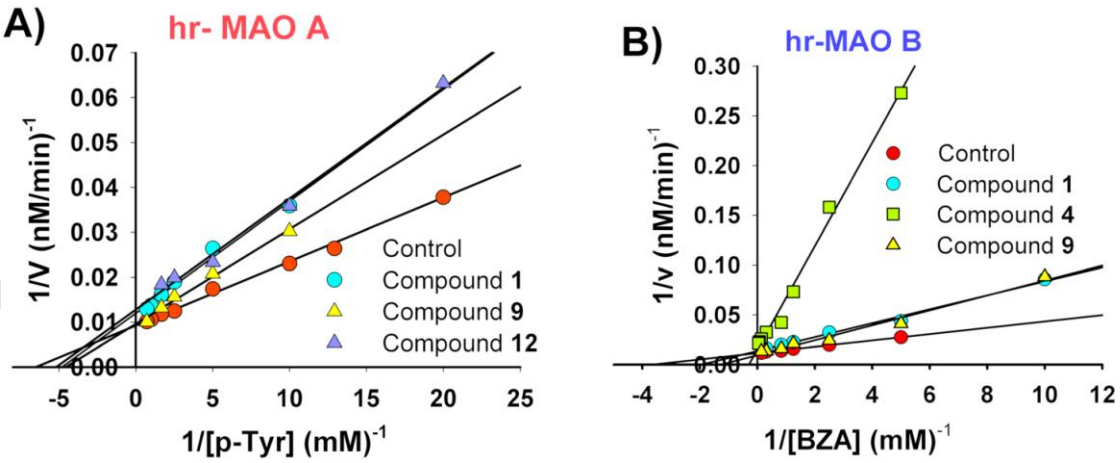

Fig. 2. Effect of compounds **1**, **4**, **9** and **12** on kinetic parameters (K_m and V_{max}) of hr-MAOs. Lineweaver-Burk plots of oxidative deamination of substrate catalysed by hr-MAO A (A) and hr-MAO B (B), in the absence (●) and presence of 100 μM compounds **1** (●),**4** (■), **9** (▲) or **12** (▲). Steady-state kinetic experiments were carried out without pre-incubating the enzyme with the compound. Solid lines were calculated by linear-regression analysis of data ($r > 0.99$).

This article is protected by copyright. All rights reserved.

Accepted Article

Accepted Article

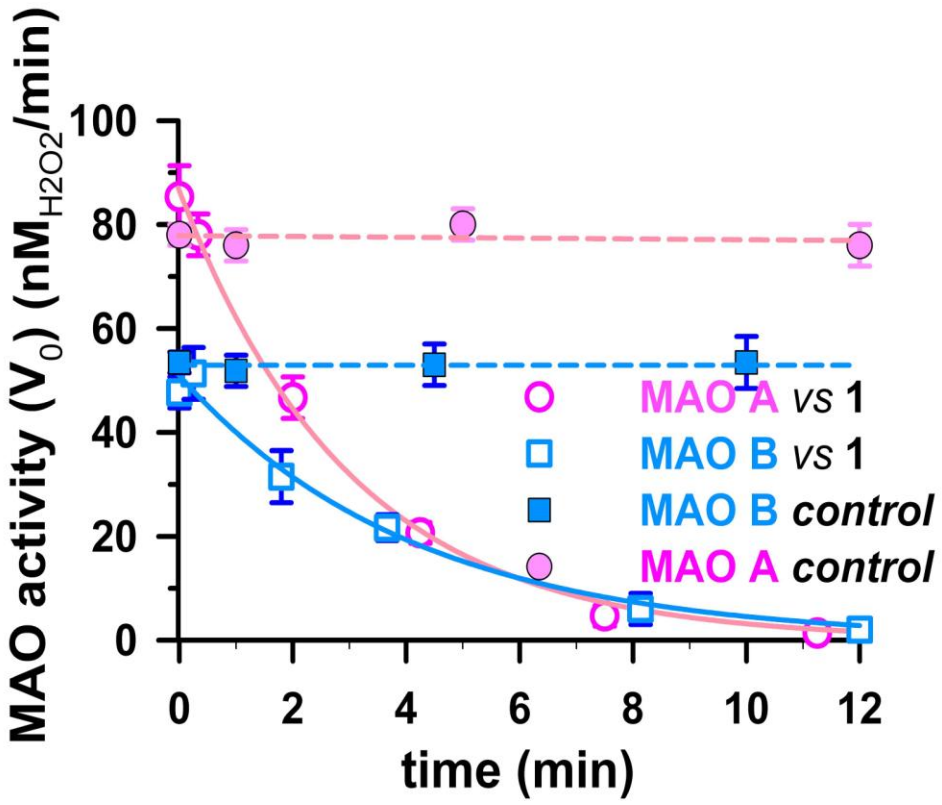

Fig. 3. Time dependent inactivation of MAOs by compound **1**
Decay of MAO activity in the presence of 100 μM compound **1** *vs* pre-incubation time; solid lines are the results of the best-fitting of the equation for an exponential decay at two parameters ($V_{(t=0)}$ and k_{obs}') to the experimental data (non-linear regression analysis, with Sigma Plot software, version 9.0; $r \geq 0.99$). No decay of MAO activity was found in control samples (dashed lines).
p-Tyr 1 mM and BZA 10 mM were used as substrate to assay the residual MAO A and MAO B activity, respectively. Error bars represent the S.D. of the data (n = 3 replicates).

This article is protected by copyright. All rights reserved.

Accepted Article

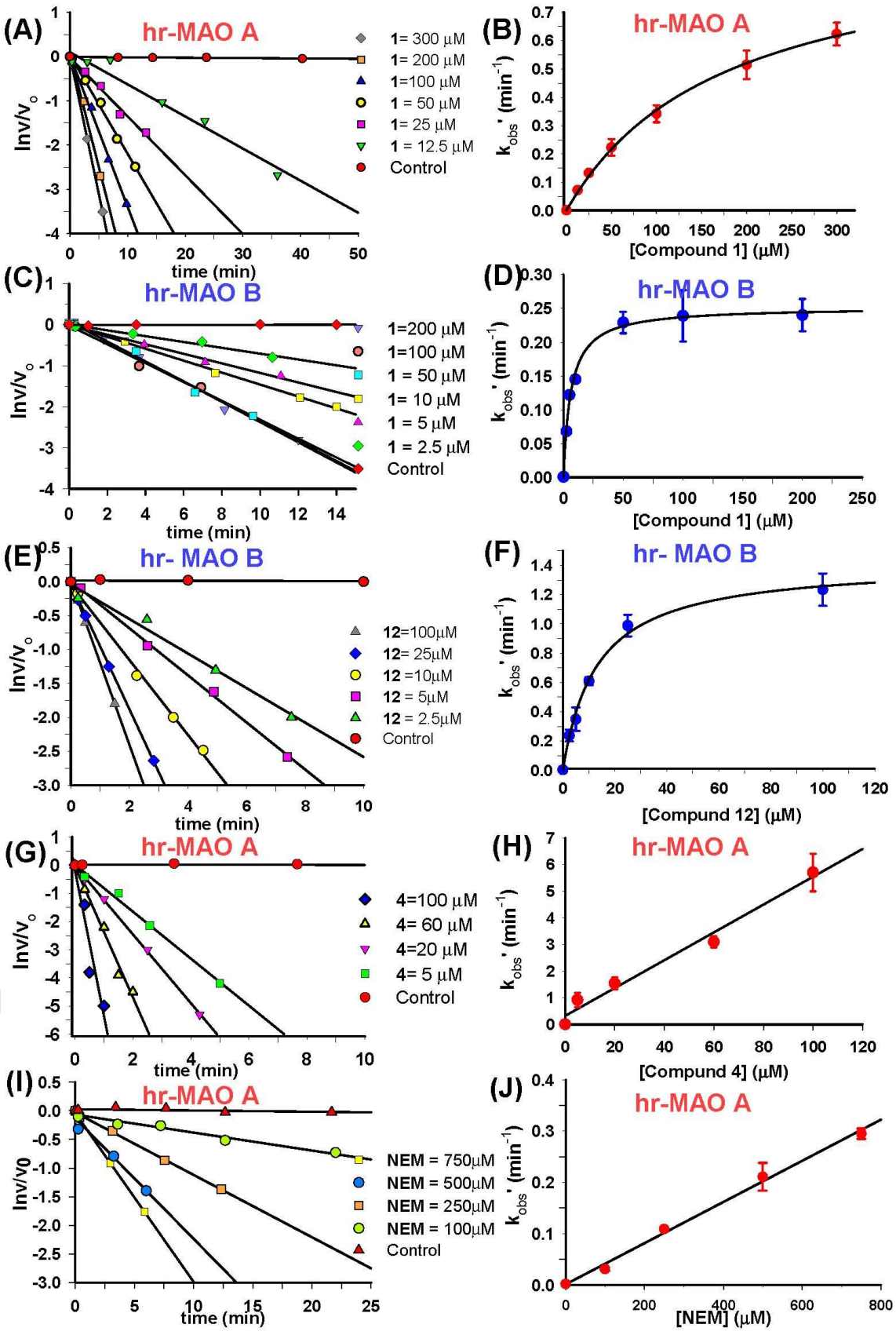

This article is protected by copyright. All rights reserved.

Fig. 4. Time and concentration-dependent inactivation of MAOs by compound **1**, **4, 12** and NEM.
Plots of logarithm of residual MAO A and MAO B activity *versus* pre-incubation time at various concentration of the different compounds: MAO A *vs* compound **1** (panel A), **4** (panel G) and NEM (panel I); MAO B *vs* compound **1** (panel C) and compound **12** (panel E). Solid lines were calculated by linear-regression analysis of the plotted data ($r \geq 0.98$); the slope values of each straight line are the apparent inactivation rate constant of MAO (k_{obs}') at the given inhibitor concentration.
The secondary plots of the calculated k_{obs}' of MAO A (panels B, H, L) and MAO B (panels D and F) as a function of compound concentrations. Fitting the Kitz-Wilson equation (eqn. 2) to plotted data (continuous line, in panels B, D and F), the inactivation rate constant (k_{inact}) and the inhibition constant (K_{IE}) were calculated. In panel H, the plot of k_{obs}' of MAO A *vs* **4** concentration shows the linear-behaviour of this compound in the explored concentration range: from the slopes of this plots $k_{inact}/K_{IE} = 51 \pm 7 \times 10^3$ min^{-1} M^{-1} was calculated for compound **4** *vs* MAO A. A similar behaviour was found for MAO A *vs* NEM ($k_{inact}/K_{IE} = 400 \pm 46$ min^{-1} M^{-1}, from the slope of the plot in panel J). The residual MAO A and MAO B activity *versus* pre-incubation time with the different compounds was assayed using *p*-Tyr 1 mM and BZA 10 mM as substrates for MAO A and MAO B, respectively. Error bars represent the S.D. of the parameters (n = 3 replicates)

This article is protected by copyright. All rights reserved.

Accepted Article

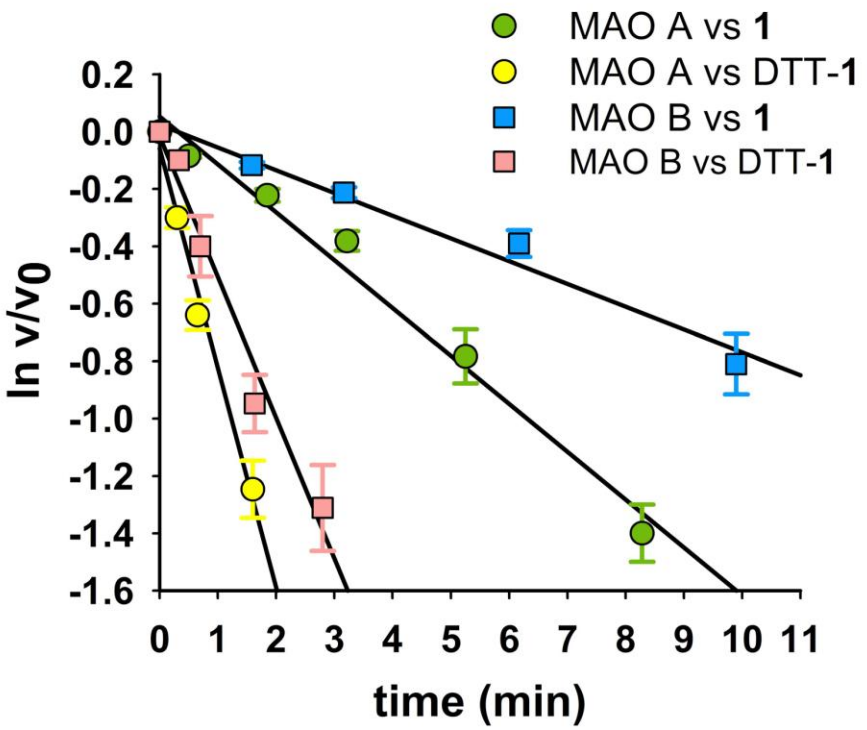

Fig. 5. Effect of DTT on inactivation properties of compound **1** *vs* MAOs.
Plots of logarithm of residual MAO activity *versus* pre-incubation time with 100 μM compound **1** (MAO A (●) and MAO B (■) or 100 μM compound **1** after pre- reduction with DTT (MAO A (●) and MAO B (■). *p*-Tyr 1 mM and BZA 10 mM were used as substrates to assay the residual MAO A and MAO B activity, respectively. Solid lines were calculated by linear-regression analysis of data ($r \geq 0.99$); the slope values of each straight line are the apparent inactivation rate constant of MAO (k_{obs}') at the given inhibitor conditions. Error bars represent the S.D. of the data (n = 3 replicates).

This article is protected by copyright. All rights reserved.

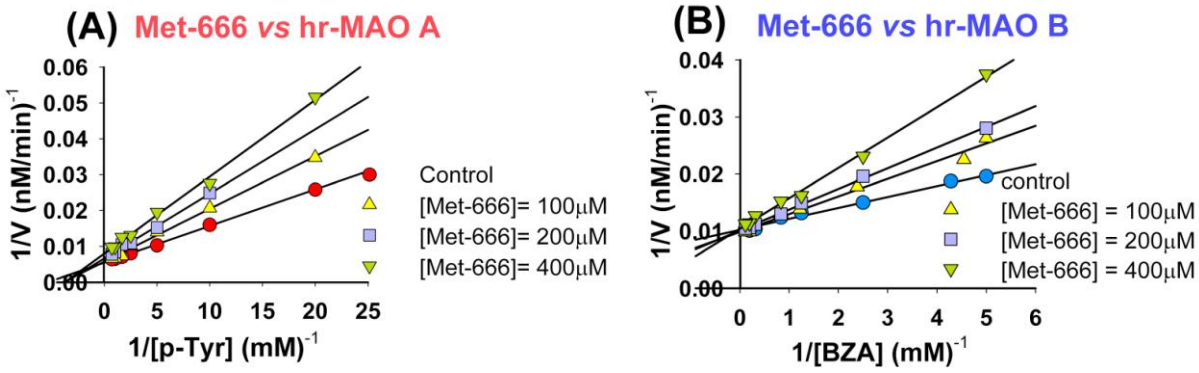

Fig. 6. Lineweaver-Burk plots of hr-MAOs activity in the presence of various concentrations of Met-666.

Steady-state kinetic experiments were carried out without pre-incubating the enzyme with the compound. (A) Double-reciprocal plots of MAO A activity. From the re-plot of apparent $Vmax_{Met\text{-}666}/Vmax_0$ values on [Met-666], K_{EI} = 790± 190 µM was calculated. A small decrease on $Km_{Met\text{-}666}$ was also observed (K_I>1mM). (B) Double-reciprocal plots of MAO B activity. From the re-plot of apparent $Km_{Met\text{-}666}/Km_0$ values on [Met-666], K_{EI} = 540 ± 130 µM was calculated. Solid lines were calculated by linear-regression analysis of data ($r \geq 0.99$).

This article is protected by copyright. All rights reserved.

Accepted Article

Accepted Article

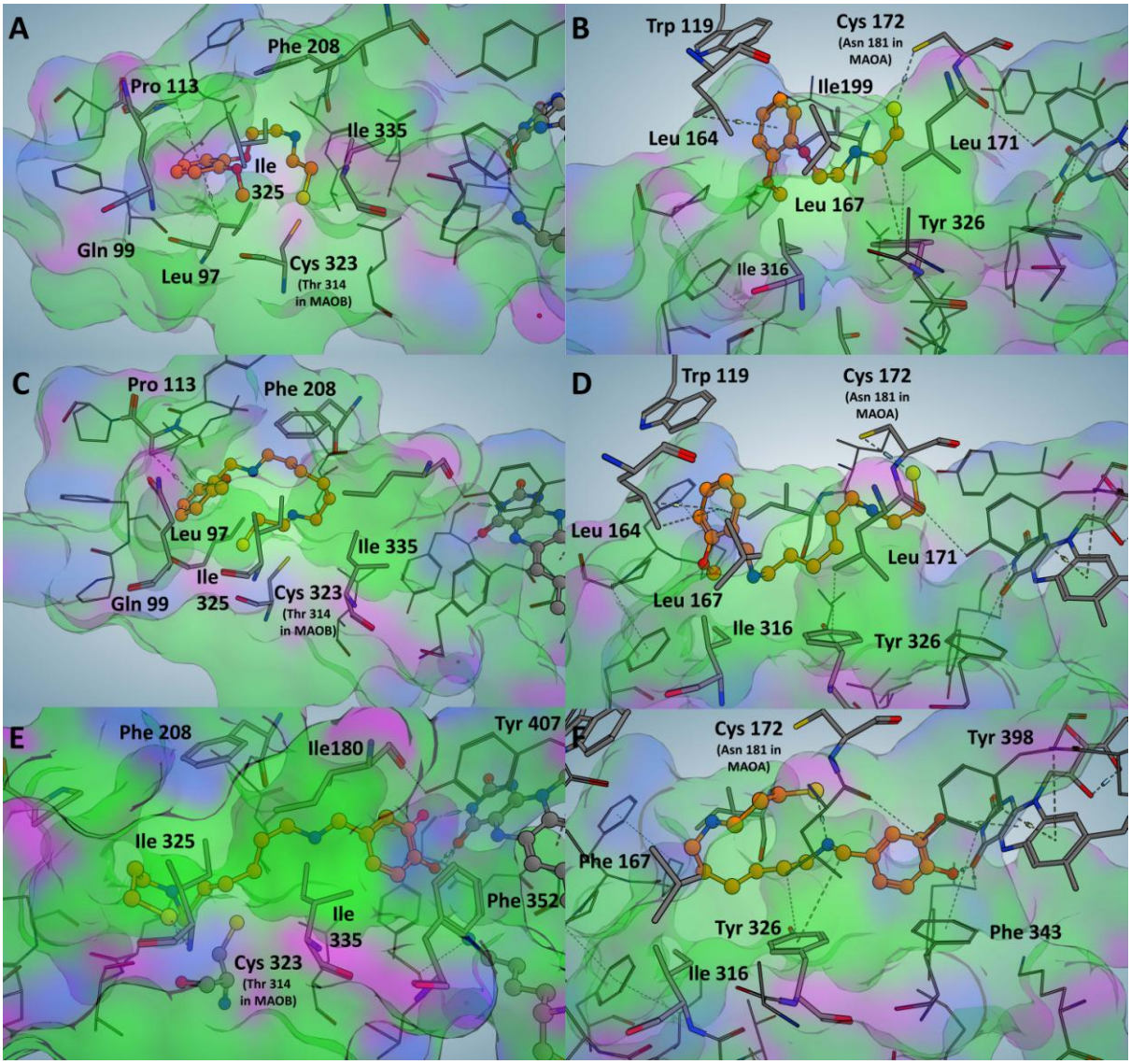

Fig. 7. Docking pose of compounds **1**, **9** and **12** against MAO A and MAO B. Compound **12** against MAO A (A) and MAO B (B); compound **1** against MAO A (C) and MAO B (D); compound **9** against MAO A (E) and MAO B (F). The most important amino acids are highlighted. The Analytic Connolly surface of MAO A and MAO B tunnels were also calculated; green and blue/violet indicate hydrophobic and hydrophilic properties, respectively.

This article is protected by copyright. All rights reserved.

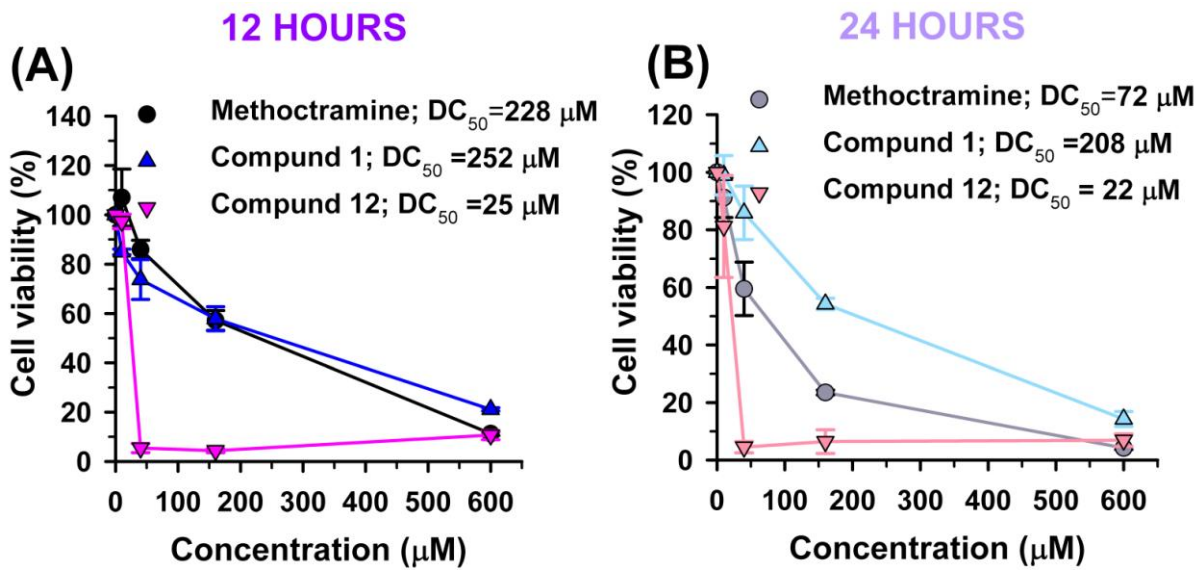

Fig. 8. Cellular effects of methoctramine and compounds **1** and **12** at 12 and 24 hours after treatments.
SH-SY5Y cells were treated for 12 h (A) and 24 h (B) with increasing concentrations of methoctramine or compound **1** or compound **12**, as indicated. Cell viability was assessed by means of MTT assay, assigning 100% value to the vehicle-treated control cells. Means ± S.D. of at least three independent experiments are shown. DC_{50} values were calculated by using the GraphPad Prism program.

This article is protected by copyright. All rights reserved.

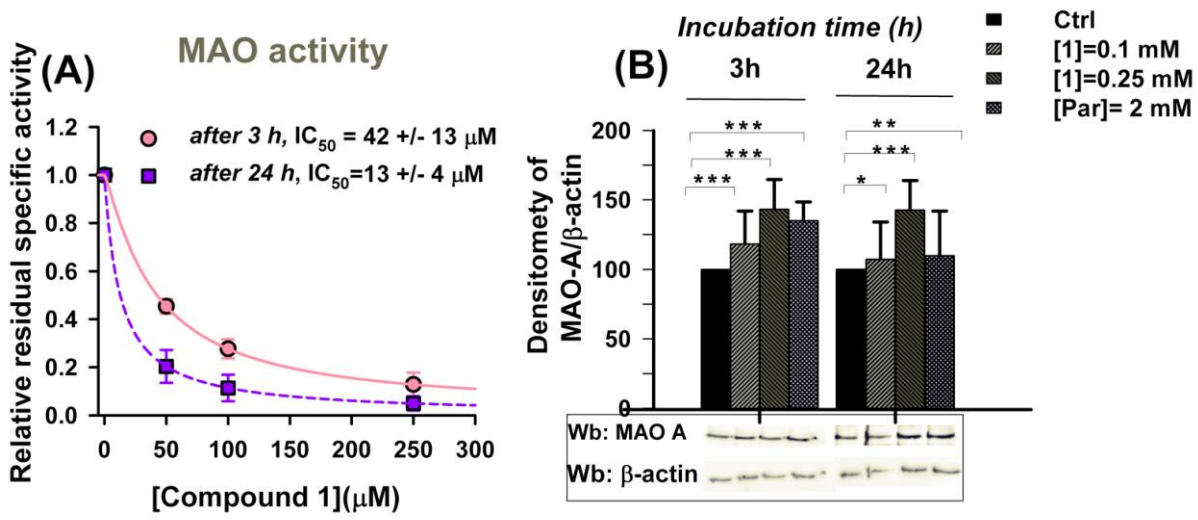

Fig. 9. Compound **1** *vs* MAO in SH-SY5Y neuroblastoma cells.
*A) Effect of compound **1** on MAO activity in SH-SY5Y cells.*
MAO activity was tested using the kynuramine assay method. Cells were treated for 3 and 24 hours with compound **1** 0, 50, 100, 250 μM or Par 2 mM before the determination of residual MAO activity in the cellular lysates. Residual MAO activity after Par treatments were 7 and 0.4% after 3 and 24 h, respectively (data not shown). Control MAO activity = 89 pmol min^{-1} $mg_{protein}^{-1}$.
Means ±S.D. of at least three independent experiments are show; IC_{50} ±S.E. values are reported.
*B) Effect of compound **1** on MAO protein in SH-SY5Ycells.*
Western blots, immuno-staining and quantitative determination of MAO A protein in SH-SY5Y cells lysates after treatment with 0, 100, 250 μM compound **1** and 2 mM Par. The values were presented as the relative ratio to untreated control. The column and bar represent the mean and S.D. of three experiments. Statistical analysis of treated cells in comparison to untreated control was carried out using analysis of variance (ANOVA) followed by Bonferroni post-test. *p<0.05, ** p<0.01 and ***p<0.001 indicate a significant difference between control and compound **1** or Par-treated cells at 3 and 24 hours.

This article is protected by copyright. All rights reserved.